Molecular analysis of human cranial compartments with different embryonic origins

Negar Homayounfar

A thesis

submitted in partial fulfillment of the

requirements for the degree of

Masters of Science

University of Washington

2013

Committee:

Michael Cunningham

Richard Presland

Sue Herring

Tracy Popowics

Program Authorized to Offer Degree:

Oral Health Medicine

University of Washington

Abstract

Molecular analysis of human cranial compartments with different embryonic origins

Negar Homayounfar

Chair of Supervisory Committee:
Professor Michael L. Cunningham
Department of Pediatrics

The human calvaria has five major sutures (the metopic, coronal, sagittal, squamosal and lambdoid). These sutures consist of intrasutural mesenchyme (ISM) each flanked by two bones. The presence of unossified sutures facilitates fetal movement through the birth canal, as well as a growth center, allowing for brain growth. During growth of the calvaria, osteogenesis takes place at ectocranial and endocranial surfaces and the osteogenic front, the leading edge of each bone. The premature fusion of the sutures is called craniosynostosis. Although there are hundreds of studies investigating the molecular causes of craniosynostosis, the molecular mechanisms involved in the normal physiological development of each suture are not well understood.

To study the mechanisms involved in normal development one must consider that sutures may be biologically distinct from each other. Known differences include the prevalence of being involved in synostosis, the type of mutations causing premature fusion of each suture, the timing of physiologic fusion and their embryonic origins. These differences suggest the existence of distinct molecular mechanisms controlling the development of each suture. Although previous

investigations suggest that different embryonic origins of the compartments of suture complexes (ISM and two flanking bones) may account for these differences, there have not been adequate studies on human calvaria to resolve this issue.

In this study, we obtained samples from human fetal calvaria. We investigated global gene expression of cells from the frontal and parietal bones and the metopic and sagittal ISM in order to assess the presence of an expression signature related to their embryonic origins. Furthermore, using a co-culture technique we evaluated changes in the gene expression, proliferation and differentiation of cells from different cranial compartments.

This work has revealed that among the four compartments, the frontal and parietal bones have the most distinct gene expression profiles despite being of the same tissue type. We found correlated expression of two groups of genes which separate frontal/metopic compartments from parietal/sagittal compartments. Several of these genes have important roles in neural crest development. We will present data that suggest a signature of embryonic origin still exists in calvarial compartments early in the second trimester of human development. Gene expression profiling of these compartments suggests frontal/metopic versus parietal/sagittal compartments have distinct profiles related to proliferation, differentiation and extracellular matrix (ECM) production.

Table of contents:

Table of contents

Acknowledgements:

I am vey thankful to my amazing mentor, Dr. Michael Cunningham, who has always been very inspirational and caring. His continued mentorship has had a profound influence on my life and scientific development. Being his student has been a great honor.

My sincere thanks also go to Dr. Richard Presland and Jennifer Kohn, for all their support and kindness.

I would like to express my gratitude to Dr. Sue Herring and Dr. Tracy Popowics.

I am grateful for having the best labmates, Sarah Park and Christine Clarke.

Finally, thanks to my husband, Ali Nosrat, for his love and support.

Introduction

During embryonic development the craniofacial mesenchyme originates from paraxial mesoderm and neural crest.[1] The craniofacial skeleton has two components, the neurocranium giving rise to cranium and the viscerocranium forming the facial skeleton. The Neurocranium has two further subdivisions, the cartilaginous neurocranium which forms the base of cranium and the membranous neurocranium which contributes to the formation of cranial vault. In the membranous neurocranium, cranial bones are formed by membranous ossification. These flat cranial bones are divided by mesenchymal tissues or fibrous joints called sutures. The human calvaria has five major sutures (the metopic, coronal, sagittal, squamosal and lambdoid) (Figure 1). The presence of unossified sutures facilitates fetal movement through the birth canal and functions as a growth center, allowing for brain growth.[2] Osteogenesis takes place at the osteogenic front, which is the leading edge of each bone[3] as well as ectocranial bone surface.

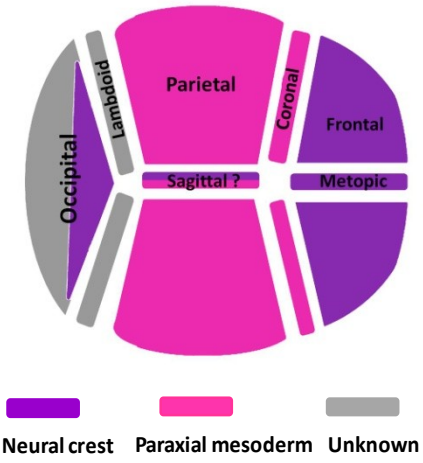

Figure 1: Major bones and sutures of human cranial vault. Different colors show embryonic origin of cranial compartments.

One of the important disorders of the cranial vault is craniosynostosis. Craniosynostosis is premature fusion of the sutures and occurs in 1/2500 of births.[4] This can cause malformations of the skull, increased intracranial pressure, and developmental delay.[5] There have been hundreds of studies on the genetic and environmental etiology of craniosynostosis. It is now known that mutations in specific genes[6], intrauterine head constriction[7-9],

hyperthyroidism[10, 11], maternal smoking[12], fertility treatment[13] and parental exposure to sodium valproate[14-16] are all associated with the pathogenesis of this disorder.

Although many studies have been performed to determine the etiology of craniosynostosis, the underlying molecular mechanisms are not yet clear. In order to achieve this goal, the basis of normal sutural development must be defined. In the study of suture biology we must consider the differences between sutural complexes i.e. ISM and two flanking bones.

Differences of cranial sutures

Suture specific prevalences of craniosynostosis

Craniosynostosis can be classified as single suture, multiple suture or syndromic synostosis. Prevalence of single suture craniosynostosis is greater than multiple suture involvement (85-95% of all cases) with the majority (50%) involving the sagittal suture. The prevalence of coronal, metopic and lambdoid synostosis is 22%, 15% and 2%, respectively.[3] The differential prevalence of synostosis in each suture suggests the existence of biologic risk factors that contribute to premature fusion.

Association of specific gene disorders to each suture synostosis

Mutations in genes encoding several growth factor receptors and transcription factors (e.g. FGFR1, FGFR2, FGFR3, TWIST1, EFNB1, FBN1, TGFBR1, RUNX2, IGF1R, MSX2 and TCF12) have been found to cause craniosynostosis [6, 17-21] however, they do not affect all the

sutures equally. In many syndromic craniosynostoses the coronal suture is the primary suture involved. Mutations of FGFR1, FGFR2 and FGFR3 in Pfeiffer, Apert, Muenke and Crouzon syndromes primarily affect the coronal suture while mutations in TWIST1 in Saethre-Chotzen syndrome can lead to coronal or sagittal synostosis.[22, 23] Duplication and quadruplication of the RUNX2 gene has been reported in isolated metopic synostosis and pan-synostosis, respectively.[18, 24]

Different origins of the compartments involved in the sutures

The embryonic origins of cranial compartments were not well understood until the work of Jiang et al.[25] Using a Cre-recombinase strategy, Jiang et al. labeled cells of neural crest origin by crossing a Wnt1-Cre mouse, that constitutively expresses Cre in cells derived from neural crest, with a reporter mouse (Rosa26) that in the presence of Cre expresses beta-galactosidase. Cre recombinase was expressed in all cells expressing Wnt1. The recombinase excised the regions flanking LacZ, and LacZ was then expressed in all cells derived from Wnt1 expressing cells. Because Wnt is expressed in the cells of neural crest origin, one could distinguish neural crest derived cells using this technique. This work demonstrated that the frontal bone, posterior frontal suture (equivalent to the metopic suture), the posterior tongue of this tissue, between the two parietal bones (sagittal suture), and the central portion of the inter-parietal bone are derived from neural crest while the parietal bone and coronal suture were derived from paraxial mesoderm. [25] These data were substantiated by Toshiyuka et al. using Wnt1-Cre/R26R mice to label neural crest cells and Mesp1-Cre/R26R mice to label mesodermal cells.[26] Gagan et al. studied the cellular lineage of the cranial vault in mice during the period from embryonic day 9 to

neonatal day 30. While their work supports the notion that the frontal bone and posterior frontal suture are derived from neural crest and that the parietal bone develops from paraxial mesoderm, their data suggest that the sagittal suture is of mesodermal origin rather than neural crest. Furthermore, their work suggests that the entire dura mater is of neural crest origin. However, they observed migration of parietal cells into the underlying dura mater, and similar migration of dural cells into the sagittal ISM.[27] As with previous work, Deckelbaum et al. also showed that frontal and parietal bones are derived from neural crest and paraxial mesoderm, respectively. They revealed that parietal cells can pass the coronal suture barriers and mingle with neural crest cells in the frontal area but the frontal cells do not migrate into the parietal region. [1] Taken together, this research supports the idea that the frontal bones and metopic suture are of neural crest origin while the parietal bone is derived from paraxial mesoderm. The origin of the sagittal ISM remains less clear.

Architecture and fusion time of sutures

Two other distinctions of the cranial sutures include their anatomic structure and the timing of physiologic fusion. The osteogenic fronts in the calvaria either forms overlapping sutures (coronal and lambdoid) or end-to-end sutures (metopic and sagittal).[3] In addition to this gross morphologic distinction, the timing of physiologic closure is not uniform. The metopic suture fuses between 3 and 9 months of age while the other cranial sutures, i.e. sagittal, coronal and lambdoid, fuse between 22 to 39 years of age[22, 28]

Although cranial suture complexes consist of the same tissue types, the above differences suggest that distinct molecular or positional mechanisms are controlling the development and fate of each suture.

Interaction of adjacent tissues in a suture complex

The proximity of the intrasutural mesenchyme and osteogenic front suggests that interactions between these tissues may be important in maintaining suture fusion or patency. Metopic (posterior frontal in rodents) and sagittal sutures fuse at different times with interfrontal suture fusion preceding the sagittal. There are numerous animal studies investigating the interaction of tissues in these two sutures. Levine et al. investigated the interaction of regional dura with posterior frontal and sagittal complex in vivo. They rotated the suture complex 180 degrees so that the posterior frontal was positioned on the sagittal dura and the sagittal suture was adjacent to the posterior frontal dura. This study demonstrated that the timing of suture fusion was predicted by the underlying dura rather than the original position of the suture.[29] Bradley et al. studied the interaction of the same regions in organ culture, and demonstrated that the dura of posterior frontal suture caused suture closure but dura of sagittal suture did not.[30] Roth et al. separated the dura mater and posterior frontal suture of rat using a thin barrier which inhibited fusion suggesting that a paracrine or direct interaction between the dura and the overlying suture was necessary for proper development.[31] Opperman et al. performed an in-vitro study on the interaction of the dura with the suture complex of the rat. Using a drop-well micropore system for co-culture of dura and the coronal suture complex, they demonstrated that the coronal suture only remained patent and behaved normally when it was in a co-culture with dura mater[32]

These studies revealed that interaction of dura mater and the suture complex is important in suture development and suggested that the secretion of diffusible factors rather than direct contact was responsible for the observed results.

Gene expression studies support the notion that regional dura influences overlying suture formation. Kwan et al. revealed that the gene expression profile of dura underlying the posterior frontal suture is not only different from dura of the sagittal suture but also changes before, during and after posterior frontal suture fusion.[33] Greenwald et al. investigated the expression of candidate genes and revealed that dura mater underlying the posterior frontal suture is more osteogenic than the dura of sagittal suture even before histologic fusion occurs.[34] Warren et al. obtained the same result from cell co-cultures demonstrating increased osteogenesis in osteoblasts when they interact with the cells from the posterior frontal dura.[35] Each of these studies supports the existence of regional differences in gene expression in cranial vault and that an interaction between adjacent tissues is important in suture biology.

The interactions between adjacent tissues and cells can take place through soluble factors (paracrine effect) or cell-cell contact (juxtacrine effect). Micropore drop-well systems allow the investigation of paracrine effects because they prevent cell-cell contact (juxtacrine effects) but permit the diffusion of soluble factors by sharing media. Studies on the co-culture of dural cells and the cells of suture complex in drop-well systems have demonstrated that secreted soluble factors account for these interactions.[32, 33, 36, 37] Thus, drop-well systems appear to be a reliable method to investigate the paracrine interactions of cranial compartments.

Hypothesis

Cells from cranial compartments of different embryonic origins have unique gene expression profiles and cellular characteristics, and this difference affects the interactions between adjacent compartments through a paracrine effect.

Aims

Aim1: To evaluate differential gene expression of cranial bone and ISM cell lines with different embryonic origins using microarray technology.

Aim 2: Using microarray technology, evaluate differential gene expression of cranial osteoblasts and intrasutural mesenchyme cells with different embryonic origins after co-culture interaction.

Aim 3: To evaluate cell proliferation and differentiation in cranial osteoblasts and intrasutural mesenchyme cells with different origins after their interaction in co-culture.

Methods and Materials

Study design and samples

Samples were obtained from fetal crania of 4 normal human fetuses. Their sex and age were as follows: two females 94 and 103 days, two males 97 and 98 days. Tissues were kept in DMEM medium (Life Technologies, Grand Island, NY) containing fetal calf serum and antibiotic-antimycotic supplement (penicillin, streptomycin and amphotericin B) until primary cell lines were established.

Cell expansion

All soft tissues were removed from the parietal and frontal bones including overlying scalp, pericrania, and underlying dura. Tissue pieces were cut from frontal and parietal bones and metopic and sagittal ISM. To avoid contamination with osteoblasts, ISM tissue was dissected from the central portion of each suture. Similarly, bone was harvested at least 3mm from the margin of the suture to avoid contamination with ISM. Bone and ISM tissues were cut into 2-3mm pieces and plated in 12-well plates with Dulbecco's Modified Eagle Medium, GlutaMAX (DMEM) (Life Technologies, Grand Island, NY) containing fetal calf serum and antibiotic-antimycotic supplement (penicillin, streptomycin and amphotericin B). DMEM was the medium of choice in our study because it is a basal medium and is not known to be osteoinductive. The media were changed every 3-4 days. After reaching confluence, the cells were trypsinized with tripLE Express (Life Technologies, Denmark) and passaged. After 3 passages the cells were ready for the experiments.

Co-culture

In order to simulate a paracrine interaction between cell types a drop-well co-culture technique was used (Figure 2). In this technique one cell type is plated in the well (bottom chamber) and the other cell type in the transwell (top chamber) which is suspended just above the cells in the bottom chamber. The culture surface of transwell is a porous membrane. For our experiments we used the Corning Transwell with 0.4µm pore polyester membrane insert for 6-well plates. The 0.4µm pores allow passage of secreted proteins but prevent cell-cell contact. Therefore, the cells in transwell and the cells in the well grow in close proximity (1mm), and share media and soluble factors, but they do not come in direct contact.

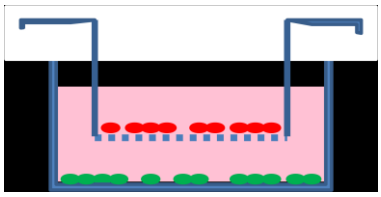

Figure 2: Drop-well co-culture

As shown in Figure 3 each cell line has a set of co-cultures consisting of 3 different interactions. Two of the co-cultures modeled the interaction of the cell line with two cell lines of a different tissue type and one is the co-culture of the cell line with itself (compartment control). Figure 3 shows four sets (frontal, parietal, metopic and sagittal) that were run for each individual. Each co-culture was performed in triplicate.

Figure 3: Frontal, parietal, metopic and sagittal sets of co-culture

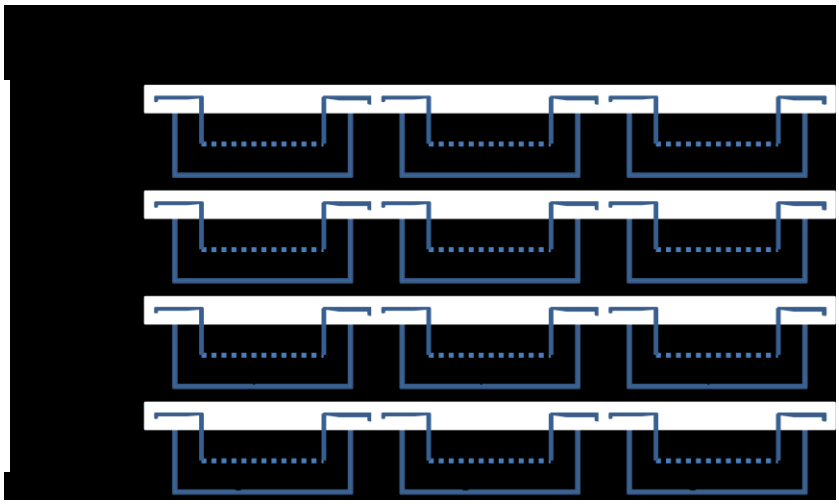

Compartment controls were used for aim 1, to compare the expression patterns of each cranial compartment.

Each of the above 12 co-cultures were performed using cell lines from each of the four fetuses. Two different culture runs were performed (each in triplicates), one for expression array and the other for measures of differentiation and proliferation.

180,000 cells were plated in each well of 6-well plates, and 90,000 cells were plated in each transwell. The differential seeding density was based on the surface area of the bottom well vs. the transwell. After plating, all the samples were incubated for 24 hours to allow cell adherence. They were then combined and co-cultured for four days before performing RNA extraction and other assays.

Co-culture for gene expression profiling

The first series of co-cultures was used to acquire RNA, perform microarray analysis and validate the results with qRT-PCR.

RNA isolation

RNA was isolated from the cells after four days of co-culture to evaluate gene expression. The cells were trypsinized, centrifuged and washed. RNA was isolated from the cells using Roche High pure miRNA Isolation Kit (Indianapolis, IN) according to the manufacturer's protocol. In order to reduce the effects of biologic and technical variability, RNA of triplicate wells was isolated separately and then mixed to have one RNA sample for microarray. Agilent 2100 Bioanalyzer was used to evaluate the integrity of RNA (Figure 4). All the RNA samples were of high quality (RNA integrity number>9). The samples were quantified with Nano Drop 1000 spectrophotometer.

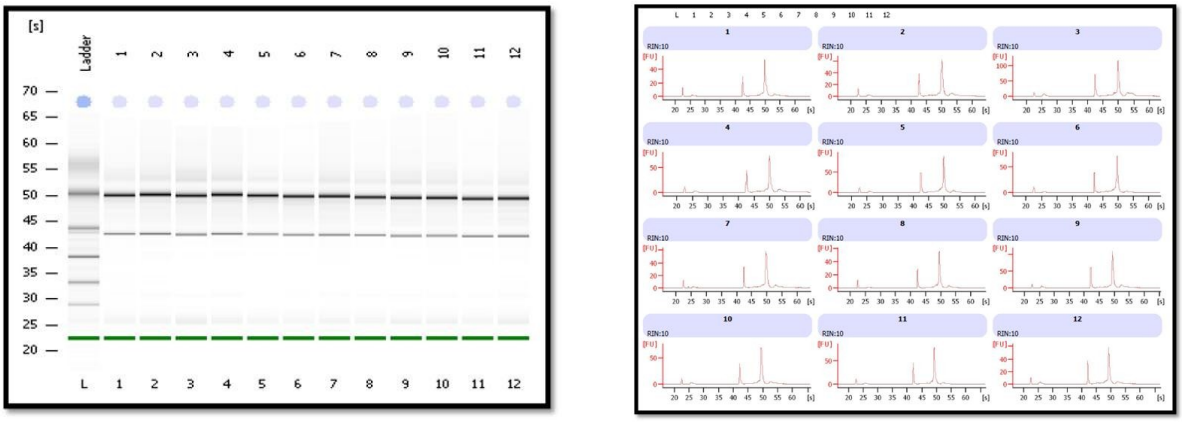

Figure 4: Separation of 28S and 18S rRNA and their ratio demonstrates good quality of RNA samples.

Microarray analysis

Microarray technology is a frequently used method to perform global gene expression profiling. In our study we used Affymetrix HuGene 2.0 ST arrays. These arrays contain DNA probes for 28,500 full-length transcripts, which include all the mRNAs produced by human genes. Chip hybridization and scanning of our samples was carried out at the University of Washington's Center for Ecogenetics and Environmental Health microarray facility.

After each sample RNA was isolated, quality checked, and quantified it was used for the preparation of fluorescent cDNA for chip hybridization. Labeled cDNA was applied to microarray chips and hybridized with the complementary strand on the chip. Fluorescence intensity was measured with a microarray scanner and signal intensity was used to calculate the relative magnitude of gene expression.

qRT-PCR validation

After statistical analysis of the expression array results, four of the genes were chosen for RT-PCR validation; TFAP2A, TFAP2B, ASXL3 and FOXF2 (see page 28). PCR primers for these genes were chosen from the primer bank of The Center for Computational and Integrative Biology of Harvard University (http://pga.mgh.harvard.edu/primerbank/). Length, melting temperature, GC content and potential secondary structure of the primers were evaluated (www.sigmaaldrich.com). They were made by Sigma-Aldrich, St Louis MO (Table 1). The primers were optimized using different concentrations of primers and pooled cDNA. The best concentrations were chosen based on the characteristics of their PCR reaction (such as efficiency and dissociation curve). Using the same RNA source for the microarray analysis, cDNA was prepared with a Thermo Scientific RevertAid First Strand cDNA Synthesis Kit according to the manufacturer's protocol. Primers were optimized and qRT-PCR was performed using SensiMix SYBR low-ROX kit (Bioline, Taunton MA) and Applied Biosystems 7500 Fast real time PCR system. PCR amplification was done in three heat cycle steps followed by a dissociation step (Table 2). 18S rRNA was used as an internal control for normalization.

Table 1: qRT-PCR primers

TFAP2A	Forward	CTCCGCCATCCCTATTAACAAG
	Reverse	GACCCGGAACTGAACAGAAGA
TFAP2B	Forward	TTCCTCCCAAATCGGTGACTT
	Reverse	CGCCGGTGTTGACAGACAT
ASXL3	Forward	ATTAGCCTGTCTGAATGCAATGC
	Reverse	GACTAAATCCAACGTGCCATCT
FOXF2	Forward	CCGTTACCAGCATCACTCTACT
	Reverse	CGCAGGGCTTAATATCCTGACA
18S	Forward	CATTAAATCAGTTATGGTTCCTTTGG
	Reverse	CCCGTCGGCATGTATTAGCT

Table 2: qRT-PCR cycle parameters

qRT-PCR	Stage 1	Stage 2	Stage 3		Stage 4		
rep:	1	1	40		1		
Heat (◦C):	50	95	95	60	95	60	95
Duration (min):	2	10	15	1	15	1	15

Co-culture for proliferation and differentiation assays

The second set of co-cultures (6-well plates) were used for proliferation and differentiation assays. On day 3 of the co-culture bromodeoxyuridine (BrdU, see details below) was added to the wells. On day 4, the cells were trypsinized and counted using hemacytometer. In order to transfer the cells to 96-well plates, 1/10 of the volume of the media containing cells was added to each well. Two 96-well plates were prepared for proliferation and differentiation assays. Each cell line was plated in triplicate.

Cell proliferation assay

BrdU Cell Proliferation kit (Millipore, Temecula CA) was used for proliferation evaluation. Bromodeoxyuridine (BrdU) is an analog of thymidine and during the cell cycle it is incorporated in the newly synthesized DNA strands by replacing thymidine. BrdU is detectable by immunochemical means and is routinely used to measure cellular proliferation.

The 96-well plates prepared for this assay were treated according to the manufacturer's protocol for cells in suspension. The 96-well plates were spun down; the media was removed and the cells were fixed. Anti BrdU mouse monoclonal antibody, goat antimouse Ig-peroxidase, substrate and stop solution were added as per protocol. Optical density (OD) was read at 450 nm using a spectrophotometer microplate reader and used to calculate relative proliferation.

Differentiation assay

We used Alkaline Phosphatase Yellow (pNPP) Liquid Substrate (Sigma- Aldrich, St Louis MO) to measure differentiation. Para-Nitrophenylphosphate is a chromogenic substrate for alkaline phosphatase.

After spinning down the second 96-well plate (designated for differentiation assay) the media was removed and the cells were gently washed with PBS. pNPP was added, incubated, and stopped by adding NaOH. OD was read at 405 nm in a spectrophotometer. In order to control for the effect of proliferation the relative differentiation of each sample was calculated by the

measured OD normalized to cell number. This value was used to compare the relative differentiation of different cell cultures.

Analyses

Microarray analysis

The raw data were normalized, background corrected, and then summarized using a robust multi-array average. A weighted analysis of variance (ANOVA) model was fit to the data that included factors for sample type, gender, and a blocking factor to account for intra-subject samples. Then all needed comparisons were made using empirical Bayes adjusted contrasts. This is very similar to computing t-statistics, power was gained here to detect true differences.[38-40]

qRT-PCR analysis

The fold changes were calculated by the standard ΔΔCt method. In this method it is assumed that the efficiency of amplification is close to 100% and the amount of cDNA is doubled by each heat cycle (Ct). Therefore when the cDNA amplicons of two samples reach a certain level (number) the difference in the number of heat cycles needed to reach that level (ΔΔCt) indicates the relative amount of each cDNA. Before calculating ΔΔCt, the Ct of each sample is normalized using the Ct of 18S (ΔCt). Fold change of the expression of a gene in two samples is obtained by calculating 2^(- ΔΔCt).

Expression correlation analysis

Singular value decomposition (SVD), a matrix factorization method, was used to analyze microarray data.[41, 42] An SVD of a matrix breaks the variation into the following discrete components: Patterns across genes (eigenarrays); Pattern across samples (eigengenes); and weights describing the relative importance of each eigenarray/eigengene, (eigenweights). One of many benefits of SVD is that it can be used to hone in on the most important sources of variation present in the data. This is especially useful for high-dimensional genomic data with large amounts of dependence between genes and samples (dependence here meaning highly correlated data for genes involved in similar pathways and between samples that are biological replicates of similar conditions). The general strategy for making use of an SVD of a matrix is to first inspect the eigenweights to determine the number of important variables, then investigate the corresponding eigenarrays or eigengenes to learn more about the importance of various genes, pathways or groups of samples. This approach was followed for our data and two eigenweights were identified significantly larger than the remaining. Clustering the first two eigenarrays suggested the existence of three distinct groups of genes. Their corresponding patterns across the samples were used to define three distinct eigenpatterns or consensus patterns across samples. The 3 groups of genes and consensus patterns were then investigated further.

Results

Microarray results

Paired comparison of fold changes (standard pairwise comparison)

Comparison of controls

In order to compare the gene expression of different compartments the expression of compartment controls (the same cells grown in the top and bottom of the transwell) was compared in pairs. Six paired comparisons were made between four compartments (Figure 5).Fold changes larger than 1.5 and smaller than -1.5 (p-value < 0.05) were considered significant.

Table 3 shows the number of differences in each comparison. Tables S1 to S6 show statistically significant differences of these comparisons. Frontal vs. parietal bone cultures exhibited the largest number of differentially expressed genes (Table 3). On the other hand, frontal bone vs. metopic ISM and parietal bone vs. sagittal ISM had the smallest numbers.

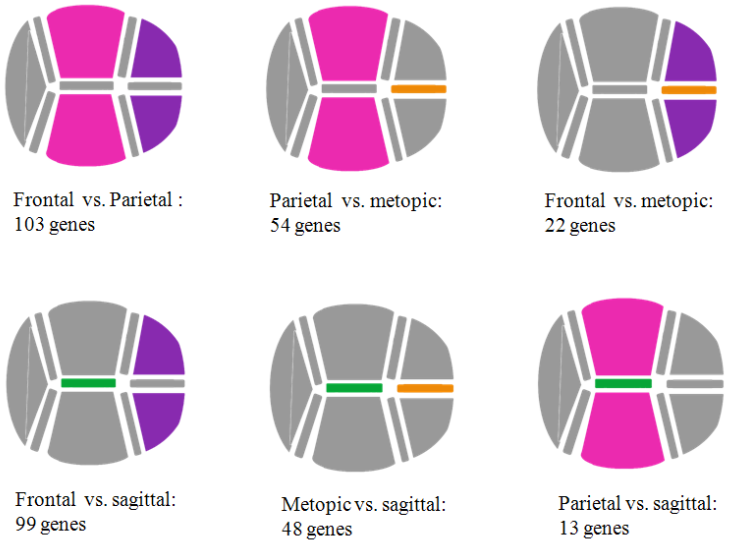

Figure 5: Number of differentially expressed genes in each comparison

Table 3: Number of differentilly expressed genes in comparisons of compartments

comparison	count
Frontal vs. Parietal	103
Frontal vs. Sagittal	99
Parietal vs. Metopic	54
Metopic vs. Sagittal	48
Frontal vs. Metopic	22
Parietal vs. Sagittal	13

Comparison within co-culture set

We also evaluated the changes in gene expression of cells from each compartment when grown in co-culture conditions with other tissue types. In order to do so, we compared the gene expression of the cells in co-culture versus control cells.

Among all four co-culture sets (frontal, parietal, metopic and sagittal), the frontal set (i.e. co-culture of frontal cells with metopic and sagittal cells) had more differentially expressed genes

when compared to the control. Within this set, the frontal cells in co-culture with sagittal cells had the largest number of significantly altered transcripts when compared to control. Tables S7 and S8 show the comparison of gene expression in co-cultured frontal cells and control frontal cells. None of the other co-culture sets demonstrated more than one significantly altered mRNA. No further analysis was performed on these co-cultures.

Transcript correlation analysis

Transcript correlation analysis revealed that 795 of the genes represented in our array had correlated expression in cranial compartments (Figure 6). 264/795 genes (Group 1) had relatively high expression in frontal bone and metopic ISM (Figure 7, Table S9) compared to parietal bone and sagittal ISM. In contrast, 394/795 genes (group 2), were expressed more in parietal/sagittal compartments (Figure 8, Table S10). 137/795 genes (Group 3), were upregulated in metopic and sagittal intrasutural mesenchyme (Figure 9, Table S11). The significant overlap in gene expression in group 3 (Figure 9) demonstrated that differential expression of group 3 genes between compartments was not as large as in group 1 or 2.

Figure 6: 795 genes had correlated expression through out all the microarrays

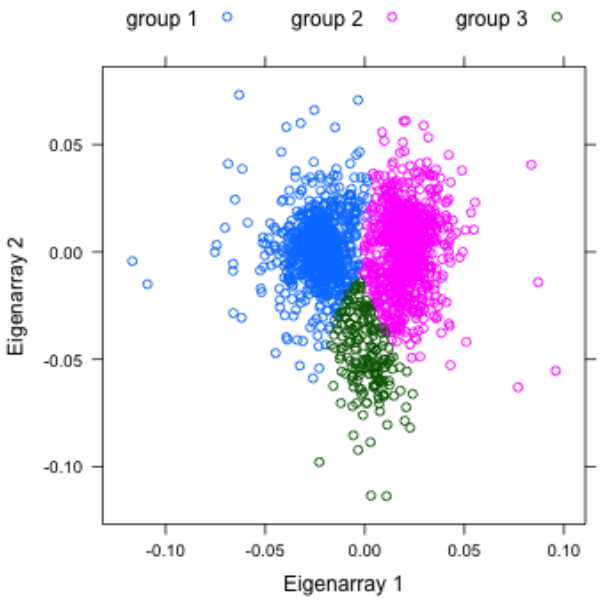

Figure 7: Correlated genes in group 1, highly expressed in frontal and metopic compartments

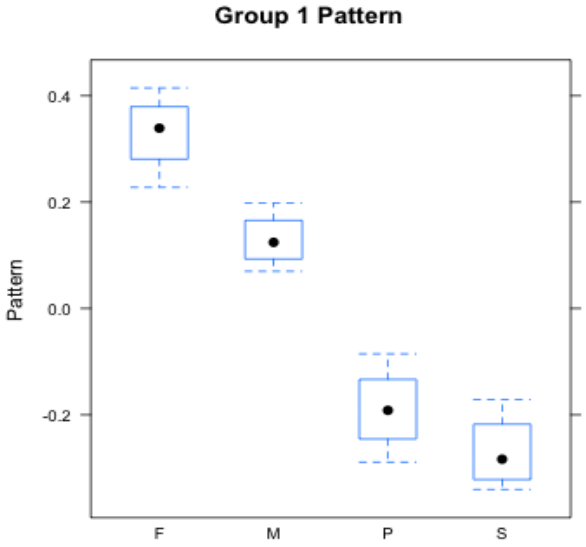

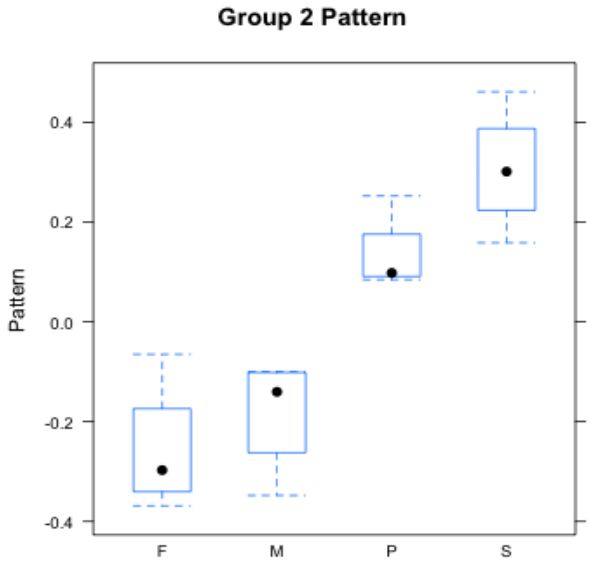

Figure 8: Correlated genes in group 2, highly expressed in parietal and sagittal compartments

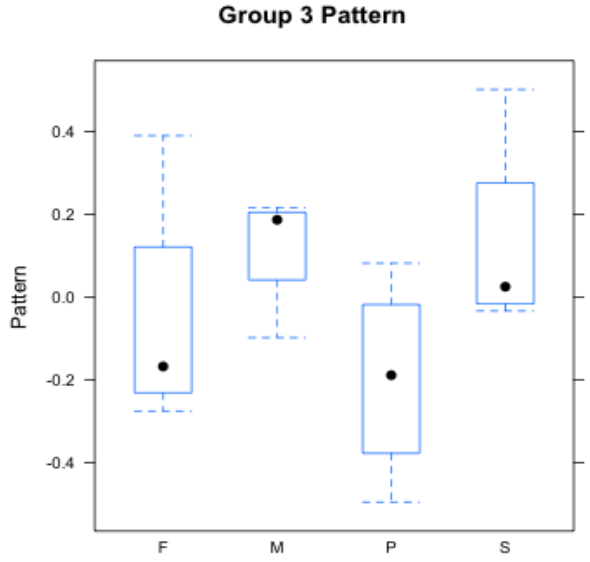

Figure 9: Correlated genes in group 3, highly expressed in metopic and sagittal compartments

The analysis described above was performed on compartment controls (the same cells grown in the transwell and bottom well). Correlation analysis was also performed on the results from the

sets of co-cultures (the cells under the influence of other types of cells). The analysis of these co-cultures did not reveal any modules with correlated genes so no further analysis was pursued.

Combining the results from two analyses

Correlation analysis revealed three gene groups (Group 1, 2, 3). Group 1 and 2 were found to be defined by correlations between frontal/metopic and parietal/sagittal gene expression profiles and group 3 was defined by correlation of metopic/sagittal suture gene expression. The correlation structures were defined independent of statistical significance, therefore we combined the results of two analyses to identify genes which are highly correlated and significantly different in expression level. This combined analysis of the results related to group 1 and 2 is shown in Table 4 and 5. In order to be included in these lists, the gene had to be significantly different in four comparisons of frontal/metopic versus parietal/sagittal compartments and also not demonstrating significant differences between frontal versus metopic or parietal versus sagittal comparisons. The same was performed for gene group 3. Similarly, each genes had to be significantly different in four comparisons of frontal/parietal and metopic/sagittal compartments and insignificant in comparisons of frontal versus parietal or metopic versus sagittal. None of the genes in group 3 met this requirement. Therefore, no further analysis was performed on this group.

This approach was used to enrich for genes with differential expression between compartments of different embryonic origin. Obviously, this inclusion criterion was very restrictive and made the gene lists very short. For that reason we relaxed our statistical analysis to include transcripts

with greater than 20% change in expression level with a p-value of ≤ 0.05 in order to allow an adequate number of transcripts for pathway analysis.

Validation results

Among the genes present in Tables 4 and 5 TFAP2A, TFAP2B, ASXL3 and FOXF2 were chosen for validation for to two reasons: (1) These are the only transcription factors that met our analysis criteria. Since transcription factors can affect the expression of a wide range of genes, finding differences in their expression may lead to better understanding of expression variation of other genes and (2) each of these genes is important in neural crest development and in some cases cause craniofacial disorders when mutated.[43-46] qTR-PCR of these transcripts validated our microarray results (Table 6).

Table 6: qRT-PCR validation result

symbol	F_F-P_P foldΔ	P-value	F_F-S_S foldΔ	p-value	M_M-P_P foldΔ	p-value	M_M-S_S foldΔ	p-value	F_F-M_M foldΔ	p-value	P_P-S_S foldΔ	p-value
TFAP2B	19.65	2.4E-02	34.76	1.7E-03	30.93	2.0E-02	54.71	2.4E-03	-1.57	4.7E-01	1.77	6.3E-01
TFAP2A	6.48	5.9E-03	5.4	7.0E-03	6.54	1.6E-03	5.45	1.6E-03	-1.01	9.8E-01	-1.2	5.6E-01
ASXL3	1.34	5.1E-01	2.3	1.4E-01	2	1.6E-01	3.42	5.0E-02	-1.49	4.8E-01	1.71	2.3E-01
FOXF2	-2.8	5.7E-05	-1.91	6.0E-04	-2.23	6.7E-03	-1.52	7.5E-02	-1.25	2.6E-01	1.46	2.3E-02

Table 4: Correlated genes, highly expressed in frontal and metopic compartments (table is sorted based on frontal-parietal fold change)

symbol	gene name	unigene	F_F-P_P foldΔ	p-value	F_F-S_S foldΔ	p-value	M_M-P_P foldΔ	p-value	M_M-S_S foldΔ	p-value	S_S-P_P foldΔ	p-value	F_F-M_M foldΔ	p-value
TFAP2B	transcription factor AP-2 beta (activating enhancer binding protein 2 beta)	Hs.33102	3.78	7.6E-04	4.52	1.8E-04	5.85	2.1E-05	7	4.4E-06	0.84	6.2E-01	0.65	2.3E-01
MAB21L1	mab-21-like 1 (C. elegans)	Hs.584776	3.68	1.1E-03	2.32	2.8E-02	3.87	7.4E-04	2.44	2.0E-02	1.58	2.2E-01	0.95	8.9E-01
MTRNR2L2	MT-RNR2-like 2	Hs.666077	3.07	7.5E-05	3.07	7.3E-05	2.13	4.7E-03	2.13	4.6E-03	1	9.9E-01	1.44	1.6E-01
DNAJC6	DnaJ (Hsp40) homolog, subfamily C, member 6	Hs.647643	2.6	5.9E-05	2.45	1.4E-04	2.5	1.1E-04	2.35	2.5E-04	1.06	7.8E-01	1.04	8.5E-01
FAM105A	family with sequence similarity 105, member A	Hs.477887	2.06	2.8E-03	1.69	2.5E-02	2.52	2.2E-04	2.07	2.7E-03	1.22	3.9E-01	0.82	3.8E-01
DRAM1	DNA-damage regulated autophagy modulator 1	Hs.525634	1.92	3.2E-03	1.98	2.2E-03	1.79	8.1E-03	1.84	5.7E-03	0.97	8.9E-01	1.08	7.3E-01
MRAP2	melanocortin 2 receptor accessory protein 2	Hs.370055	1.88	3.0E-02	2.06	1.4E-02	2.21	7.3E-03	2.43	3.1E-03	0.91	7.5E-01	0.85	5.6E-01
DNER	delta/notch-like EGF repeat containing	Hs.234074	1.84	1.5E-02	1.78	2.2E-02	1.73	2.7E-02	1.67	3.8E-02	1.04	8.9E-01	1.06	8.1E-01
IVNS1ABP	influenza virus NS1A binding protein	Hs.497183	1.73	1.1E-03	1.55	7.8E-03	1.74	1.1E-03	1.55	7.8E-03	1.12	4.7E-01	1	1.0E+00
PPAPDC1A	phosphatidic acid phosphatase type 2 domain containing 1A	Hs.40479	1.72	2.4E-03	1.45	3.1E-02	1.9	4.3E-04	1.61	7.0E-03	1.18	3.2E-01	0.9	5.4E-01
MT1F	metallothionein 1F	Hs.513626	1.67	3.3E-03	1.54	1.2E-02	1.66	3.5E-03	1.54	1.2E-02	1.08	6.3E-01	1	9.9E-01
ENTPD1	ectonucleoside triphosphate diphosphohydrolase 1	Hs.722260	1.66	7.0E-03	1.65	7.9E-03	1.5	2.7E-02	1.49	3.0E-02	1.01	9.6E-01	1.1	5.8E-01
MT1X	metallothionein 1X	Hs.374950	1.65	5.6E-04	1.49	4.4E-03	1.61	9.0E-04	1.46	6.8E-03	1.1	4.6E-01	1.02	8.7E-01
GPR183	G protein-coupled receptor 183	Hs.784	1.61	5.1E-05	1.49	4.5E-04	1.44	1.2E-03	1.33	8.4E-03	1.08	4.7E-01	1.12	2.9E-01
TFAP2A	transcription factor AP-2 alpha (activating enhancer binding protein 2 alpha)	Hs.519880	1.53	1.1E-02	1.73	1.3E-03	1.74	1.2E-03	1.97	1.2E-04	0.88	4.3E-01	0.88	4.2E-01
ACADM	acyl-CoA dehydrogenase, C-4 to C-12 straight chain	Hs.445040	1.53	2.2E-02	1.5	3.0E-02	1.5	3.1E-02	1.46	4.1E-02	1.02	9.0E-01	1.03	8.9E-01
ICAM1	intercellular adhesion molecule 1	Hs.643447	1.5	7.0E-04	1.62	8.2E-05	1.26	4.3E-02	1.36	7.6E-03	0.92	4.7E-01	1.19	1.2E-01
KRT7	keratin 7	Hs.411501	1.49	1.7E-02	1.47	2.1E-02	1.47	2.1E-02	1.45	2.7E-02	1.02	9.2E-01	1.02	9.2E-01
ABI3BP	ABI family, member 3 (NESH) binding protein	Hs.477015	1.47	4.7E-02	1.54	2.7E-02	2.04	5.3E-04	2.13	2.6E-04	0.96	8.1E-01	0.72	9.1E-02
CDH3	cadherin 3, type 1, P-cadherin (placental)	Hs.191842	1.47	4.2E-03	1.39	1.3E-02	1.64	3.2E-04	1.56	1.2E-03	1.06	6.6E-01	0.89	3.6E-01
NGF	nerve growth factor (beta polypeptide)	Hs.2561	1.46	5.3E-04	1.37	3.5E-03	1.32	8.3E-03	1.24	4.1E-02	1.07	5.0E-01	1.11	3.2E-01
SULF1	sulfatase 1	Hs.409602	1.45	2.4E-06	1.23	3.4E-03	1.46	2.0E-06	1.24	2.9E-03	1.18	2.0E-02	1	9.5E-01
ASXL3	additional sex combs like 3 (Drosophila)	Hs.464876	1.42	4.7E-02	1.46	3.3E-02	1.73	3.1E-03	1.78	2.0E-03	0.97	8.8E-01	0.82	2.7E-01
PLAT	plasminogen activator, tissue	Hs.491582	1.42	1.5E-03	1.4	1.9E-03	1.36	4.3E-03	1.35	5.3E-03	1.01	9.4E-01	1.04	7.0E-01
MYPN	myopalladin	Hs.55205	1.42	3.8E-04	1.34	2.1E-03	1.53	3.0E-05	1.44	1.9E-04	1.06	5.5E-01	0.93	4.1E-01
IL11	interleukin 11	Hs.467304	1.37	1.8E-03	1.43	4.7E-04	1.25	2.2E-02	1.31	6.9E-03	0.96	6.4E-01	1.1	3.4E-01
IGHG1	immunoglobulin heavy constant gamma 1 (G1m marker)	Hs.510635	1.35	3.2E-02	1.56	2.4E-03	1.33	4.5E-02	1.53	3.5E-03	0.87	3.0E-01	1.02	8.9E-01
LDOC1	leucine zipper, down-regulated in cancer 1	Hs.45231	1.34	2.7E-03	1.48	1.3E-04	1.26	1.7E-02	1.39	1.0E-03	0.91	3.0E-01	1.07	4.8E-01
TFAP2C	transcription factor AP-2 gamma (activating enhancer binding protein 2 gamr	Hs.473152	1.45	3.1E-02	1.42	4.3E-02	1.4	4.9E-02	1.37	6.6E-02	1.04	8.4E-01	1.02	8.9E-01

Table 5: Correlated genes, highly expressed in parietal and sagittal compartments (table is sorted based on frontal-parietal fold change)

symbol	gnee name	unigene	F_F-P_P foldΔ	p-value	F_F-S_S foldΔ	p-value	M_M-P_P foldΔ	p-value	M_M-S_S foldΔ	p-value	S_S-P_P foldΔ	p-value	F_F-M_M foldΔ	p-value
ST6GALNAC5	ST6 (alpha-N-acetyl-neuraminyl-2,3-beta-galactosyl-1,3)-N-acetylgalactosaminide alpha-2,6-sialyltransferase 5	Hs.303609	-2.08	8.0E-04	-2.28	2.1E-04	-1.52	4.3E-02	-1.67	1.5E-02	1.1	6.5E-01	-1.37	1.3E-01
C3orf62	chromosome 3 open reading frame 62	Hs.403828	-1.85	8.0E-03	-1.58	4.5E-02	-1.91	5.4E-03	-1.63	3.3E-02	-1.17	4.7E-01	1.03	8.8E-01
PDE5A	phosphodiesterase 5A, cGMP-specific	Hs.647971	-1.78	7.2E-06	-1.75	1.0E-05	-1.4	4.3E-03	-1.38	5.8E-03	-1.01	9.1E-01	-1.27	3.6E-02
HSPB6	heat shock protein, alpha-crystallin-related, B6	Hs.534538	-1.74	1.0E-03	-1.69	1.7E-03	-1.53	9.3E-03	-1.49	1.5E-02	-1.03	8.5E-01	-1.14	4.2E-01
TNC	tenascin C	Hs.143250	-1.74	1.6E-04	-1.55	1.9E-03	-2.05	3.5E-06	-1.83	5.2E-05	-1.12	3.9E-01	1.18	2.2E-01
FOXF2	forkhead box F2	Hs.484423	-1.71	8.8E-04	-1.35	4.9E-02	-1.72	7.5E-04	-1.36	4.4E-02	-1.26	1.2E-01	1.01	9.6E-01
TNFRSF11B	tumor necrosis factor receptor superfamily, member 11b	Hs.81791	-1.69	1.0E-03	-1.77	3.8E-04	-1.64	1.7E-03	-1.72	6.6E-04	1.05	7.3E-01	-1.03	8.5E-01
KLHL4	kelch-like family member 4	Hs.49075	-1.61	6.3E-04	-1.95	7.1E-06	-1.53	2.1E-03	-1.84	2.7E-05	1.21	1.5E-01	-1.06	6.7E-01
KCNT2	potassium channel, subfamily T, member 2	Hs.657046	-1.61	2.9E-05	-1.66	9.5E-06	-1.24	4.0E-02	-1.28	1.7E-02	1.04	7.2E-01	-1.3	1.2E-02
MFAP4	microfibrillar-associated protein 4	Hs.296049	-1.61	3.2E-03	-1.62	2.6E-03	-1.4	3.0E-02	-1.42	2.5E-02	1.01	9.5E-01	-1.14	3.8E-01
KIAA1107	KIAA1107	Hs.21554	-1.61	7.1E-05	-1.48	7.7E-04	-1.48	7.4E-04	-1.36	6.6E-03	-1.09	4.3E-01	-1.09	4.4E-01
ADH1B	alcohol dehydrogenase 1B (class I), beta polypeptide	Hs.4	-1.56	1.7E-02	-1.6	1.1E-02	-1.47	3.5E-02	-1.52	2.4E-02	1.03	8.7E-01	-1.06	7.6E-01
PRSS12	protease, serine, 12 (neurotrypsin, motopsin)	Hs.445857	-1.53	8.8E-04	-1.57	4.2E-04	-1.3	3.2E-02	-1.34	1.7E-02	1.03	8.0E-01	-1.18	1.7E-01
GEM	GTP binding protein overexpressed in skeletal muscle	Hs.654463	-1.51	1.7E-02	-1.53	1.3E-02	-1.53	1.4E-02	-1.55	1.1E-02	1.02	9.2E-01	1.01	9.4E-01
BTBD8	BTB (POZ) domain containing 8	Hs.676102	-1.51	5.0E-04	-1.48	8.0E-04	-1.33	1.1E-02	-1.31	1.6E-02	-1.02	8.7E-01	-1.13	2.6E-01
HECW2	HECT, C2 and WW domain containing E3 ubiquitin protein ligase 2	Hs.654742	-1.5	9.0E-03	-1.57	4.4E-03	-1.51	8.0E-03	-1.58	3.9E-03	1.04	7.8E-01	1.01	9.6E-01
FAM129A	family with sequence similarity 129, member A	Hs.518662	-1.41	1.5E-02	-1.37	2.3E-02	-1.43	1.1E-02	-1.4	1.7E-02	-1.02	8.7E-01	1.02	8.9E-01
FXYD1	FXYD domain containing ion transport regulator 1	Hs.442498	-1.39	1.2E-02	-1.45	5.5E-03	-1.31	4.0E-02	-1.36	2.0E-02	1.04	7.6E-01	-1.07	6.2E-01
CCND2	cyclin D2	Hs.376071	-1.38	1.7E-02	-1.41	1.1E-02	-1.39	1.4E-02	-1.43	9.1E-03	1.02	8.5E-01	1.01	9.4E-01
MYLIP	myosin regulatory light chain interacting protein	Hs.484738	-1.35	9.4E-03	-1.42	3.1E-03	-1.28	3.2E-02	-1.34	1.2E-02	1.05	6.7E-01	-1.06	6.1E-01
ARHGEF35	Rho guanine nucleotide exchange factor (GEF) 35	Hs.534621	-1.28	4.1E-02	-1.39	6.7E-03	-1.31	2.4E-02	-1.43	3.7E-03	1.09	4.6E-01	1.03	8.2E-01

Proliferation and differentiation results

The analysis of proliferation and differentiation assays utilized average optical density and standard deviation of each group of samples (Table 7 and 8). The results were highly variable, did not reach statistical significance, and were not felt to be reliable for further analysis.

Table 7: Optical density results of proliferation assay

BrdU		OD (nm)	stdev
Frontal set	F_F	0.363	0.363
	M_F	0.533	0.411
	S_F	0.48	0.258
Metopic set	M_M	0.605	0.563
	F_M	0.695	0.465
	P_M	0.822	0.448
Parietal set	P_P	0.22	0.415
	M_P	0.405	0.473
	S_P	0.409	0.388
Sagittal set	S_S	0.326	0.278
	F_S	0.575	0.228
	P_S	0.571	0.347

Table 8: Optical density results of differentiation assay

ALKP		OD (nm)	stdev
Frontal set	F_F	2.261	0.784
	M_F	2.383	0.927
	S_F	2.355	0.863
Metopic set	M_M	2.772	3.412
	F_M	2.255	2.394
	P_M	2.774	3.664
Parietal set	P_P	3.018	2.265
	M_P	2.986	2.682
	S_P	2.736	1.945
Sagittal set	S_S	3.422	2.077
	F_S	3.132	2.416
	P_S	3.267	1.918

Discussion

The primary goals of our study were to determine if we could detect expression signatures in cells isolated from different cranial compartments based on their embryonic origins and if these expression profiles influenced interactions between compartments. Analysis of the expression profiles of the cells from frontal and parietal bones and metopic and sagittal ISM demonstrated that the most distinct compartments are frontal and parietal bones. Based on the correlated expression of 658 genes (group 1 and 2) the compartments segregated into two groups, frontal and metopic compartments with similar expressions (higher expression of group 1 genes, lower expression of group 2 genes) and the reverse in the parietal and sagittal compartments.

We found specific biological themes in each of these groups and predict that these expression profiles confer functional differences related to the neural crest gene regulatory network (NC GRN), proliferation, differentiation, and production of extracellular matrix (Table 9). During embryonic development there are regulatory genes that have a tissue specific expression pattern in either neural crest or surrounding mesoderm tissues.[47] We identified expression profiles similar to neural crest in frontal/metopic compartments and profiles similar to mesoderm in parietal/sagittal compartments. Genes differentially expressed in frontal/metopic and parietal/sagittal groups were also distinguished by their effect on proliferation, differentiation, and their role in extracellular matrix (ECM) formation and cell adhesion.

Table 9: Genes of interest in comparison of frontal/metopic vs. parietal/saagittal compartments

symbol	unigene	F_F-P_P foldΔ	p-value	F_F - S_S foldΔ	p-value	M_M-P_P foldΔ	p-value	M_M-S_S foldΔ	p-value	S_S-P_P foldΔ	p-value	F_F-M_M foldΔ	p-value
TFAP2B	Hs.33102	3.78	7.6E-04	4.52	1.8E-04	5.85	2.1E-05	7	4.4E-06	0.84	6.2E-01	0.65	2.3E-01
TFAP2A	Hs.519880	1.53	1.1E-02	1.73	1.3E-03	1.74	1.2E-03	1.97	1.2E-04	0.88	4.3E-01	0.88	4.2E-01
ICAM1	Hs.643447	1.5	7.0E-04	1.62	8.2E-05	1.26	4.3E-02	1.36	7.6E-03	0.92	4.7E-01	1.19	1.2E-01
CDH3	Hs.191842	1.47	4.2E-03	1.39	1.3E-02	1.64	3.2E-04	1.56	1.2E-03	1.06	6.6E-01	0.89	3.6E-01
SULF1	Hs.409602	1.45	2.4E-06	1.23	3.4E-03	1.46	2.0E-06	1.24	2.9E-03	1.18	2.0E-02	1	9.5E-01
TFAP2C	Hs.473152	1.45	3.1E-02	1.42	4.3E-02	1.4	4.9E-02	1.37	6.6E-02	1.04	8.4E-01	1.02	8.9E-01
PLAT	Hs.491582	1.42	1.5E-03	1.4	1.9E-03	1.36	4.3E-03	1.35	5.3E-03	1.01	9.4E-01	1.04	7.0E-01
TNC	Hs.143250	-1.74	1.6E-04	-1.55	1.9E-03	-2.05	3.5E-06	-1.83	5.2E-05	-1.12	3.9E-01	1.18	2.2E-01
FOXF2	Hs.484423	-1.71	8.8E-04	-1.35	4.9E-02	-1.72	7.5E-04	-1.36	4.4E-02	-1.26	1.2E-01	1.01	9.6E-01

Regulatory genes expressed in neural crest and non-neural crest tissues have similar expression patterns in frontal/metopic and parietal/sagittal groups.

There are several genes expressed in neural crest and surrounding tissues that are involved in the early induction, specification and migration of neural crest cells and the development of their derivatives. Similar to developing neural crest cells [48-53], we identified higher levels of expression of TFAP2(A-C), SULF1and PLAT and lower levels of FOXF2 and TNC in frontal/metopic groups. Below we review data suggesting their roles in neural crest development and the implications of our findings with respect to suture development.

- TFAP2

Significant transcription factors in neural crest gene regulator network (NC GRN) include members of TFAP2 family. Transcription factor AP2 family has 5 members; A,B,C,D and E (or α, β, ϒ, δ and ε). Among these orthologs, TFAP2(A-C) have a high amino acid sequence similarity while TFAP2D is more divergent. [54, 55] In studies with mice, it was shown that Tfap2a, b and c are expressed in the early development of neural crest.[55-57] TFAP2A has an important role in different stages of neural crest development and is considered to be a neural crest specifier.[47, 51] Zhang et al. showed that in *Xenopus laevis* TFAP2A, B and C are

expressed in overlapping areas suggesting functional redundancy; however, mutation of each of these genes results in different phenotypes.[53]. Human mutations and animal models support a role of TFAP2 in craniofacial development. Loss-of-function mutation of TFAP2A leads to dolichocephaly and cleft palate in a condition known as branchio-oculo-facial syndrome.[43] Loss-of-function mutations in TFAP2B cause Char syndrome associated with a broad forehead and hypertelorism (increased distance between eyes), among other craniofacial features.[44, 58] Also, Tfap2a knock-out mice develop anencephaly, craniofacial dysmorphism due to deformed or absent ventral craniofacial bones and neural tube defects.[59, 60]

These studies report that TFAP2A-C have functional overlap in different stages of neural crest development. Strikingly, in our study, TFAP2A, B and C demonstrate high expression in the frontal/metopic groups (tissues of NC origin) compared to parietal/metopic groups suggesting not only that they have a specific role in the development of these tissues but also supporting previous studies suggesting their origin from cranial neural crest cells.

- FOXF2

Members of the FOX family are transcription factors. They are target genes of the Hedgehog signaling pathway and have suppressive effect on WNT signaling, which is a critical component of the gene regulatory network of neural crest.[61, 62] The FOX family proteins are primarily expressed in the mesodermal layers of the embryo including the paraxial, axial, lateral and lateral splenic mesoderm.[63] FOXF2 is one of the members of the FOX family and has a role in mesoderm dependant neural crest patterning.[61] Aitola et al. performed a thorough study on the

expression of FoxF2 in different organs of mice in different time points. They showed that FoxF2 has high expression in mesodermal mesenchyme next to the endodermal or ectodermal epithelium such as the mesodermal mesenchyme of the organs along the gastrointestinal tract, eye, tooth, lung, kidney, limb and backbone. It is highly expressed during development but reduces to low levels by adulthood.[63-65] Beside its expression in mesoderm, Wang et al. reported the expression of FOXF2 in neural crest derived tissues and the induction of cleft palate in FoxF2 knock-out mice.[52] In both humans and mouse models, mutations in FoxF2 are associated with cleft palate.[46] Taken together, these data suggest that FoxF2 is involved in the regulation of migration and patterning of neural crest cells through its expression in both neural crest and surrounding non-neural crest tissues. Our expression array data demonstrated high levels of expression of FOXF2 in the parietal/sagittal compartments as compared to the metopic and frontal compartments. These data suggest the possibility that FOXF2 plays a role in the development of cranial compartments derived from paraxial mesoderm rather than a direct effect on neural crest derivatives.

- SULF1

The SULF1 gene encodes extracellular heparan sulphate 6-0-endosulphatase. This enzyme remodels proteoglycans on the cell membranes so that neural crest cells are recognized by other neural crest cells during development. SULF1 modulates the path through which neural crest cells migrate.[66, 67]. The WNT, FGF and BMP pathways are important in the regulation of neural crest development[47, 62] and SULF1 modulates these pathways by making changes in heparan sulfate proteoglycan.[68] Our expression data demonstrated that SULF1 is highly

expressed in frontal and metopic compartments further supporting maintenance of neural crest-related transcripts in cranial compartments of neural crest origin.

- PLAT (T-PA)

PLAT (tissue plasminogen) is expressed in all the neural crest cells after their migration. Therefore, like WNT, it is used as a marker to trace neural crest cells and their derivatives.[50] Plasminogen activator is a proteinase that converts plasminogen into plasmin. Plasmin can degrade both cell membrane and extracellular matrix proteins. This serves to increase cell motility and plays a role in the migration of neural crest cells.[48, 49, 69] PLAT is highly expressed in the frontal/metopic compartments suggesting that cells in these compartments may be more migratory and further supports the persistence of neural crest transcripts in these compartments.

- TNC

Tenascin is a major extracellular matrix protein. It is important in cell adhesion, proliferation and differentiation. Although it is known to play an important role in development there are controversies surrounding its exact roles. While some studies suggest that it is secreted by neural crest cells playing a role in delamination and migration, others have provided data suggesting that tenascin has an inhibitory effect on neural crest migration.[70-72] Regardless of the exact effect of tenascin on NC migration, these studies demonstrate its importance on ECM and neural crest development. Our array results demonstrate high levels of expression of TNC in parietal/sagittal compartments relative to the other cranial compartments. These data suggest

significant differences in the expression of transcripts related to the ECM and migratory potential between the frontal/metopic and parietal/sagittal groups.

Studies on the embryonic origin of cranial vault suggest that the frontal and metopic compartments are of neural crest origin and parietal bones are derived from paraxial mesoderm.[25, 26] In frontal/metopic compartments, we have identified high levels of expression of neural crest regulatory genes which are known to be expressed by neural crest cells. In parietal/sagittal groups we have identified the increased expression of the genes expressed in non-neural crest tissues and yet important in the development of neural crest. Our results are in agreement with other studies on the origin of frontal, metopic and parietal compartments.

There is still controversy on the origin of sagittal ISM. While some studies suggest that the sagittal suture is of neural crest origin, others propose that it is derived from paraxial mesoderm.[25-27] Gagan et al. suggests that parietal and sagittal cells and the underlying dural matter undergo changes though invasion of neural crest from the dura.[27] Our data would suggest that at the beginning of the second trimester in humans, the sagittal suture and parietal bones have very similar gene expression patterns supporting a paraxial mesoderm origin.

Extracellular matrix and cell-cell contact is distinct in frontal/metopic and parietal sagittal compartments.

Neural crest cells go through different developmental stages such as induction and migration that are specific to the neural crest. ECM and cell surface proteins such as cadherins play an

important role in neural crest development. Consequently, there is strong temporal and spatial regulation of these proteins in neural crest cells and surrounding tissues.[73] Because the frontal and parietal bones and the metopic and sagittal ISM are the same tissue types, one might expect that their ECM composition would follow their tissue type (e.g. bone and ISM), our results show they are quite distinct (Table 9). This difference may be explained on the basis of tissue origin.

- ICAM1

One of the correlated genes that was expressed significantly higher in frontal/metopic compartments is ICAM1. Interestingly, ICAM1 has a binding site for TFAP-2 (also increased in its level of expression in the frontal/metopic groups).[74, 75] ICAM1 is a surface glycoprotein which regulates cell-cell contact and cell movement through ECM. [76-78] High expression of ICAM1 can be seen in skin, oral, breast, lung and bone cancer. Moreover, in many studies the magnitude of the expression of ICAM1 is correlated with the invasiveness of the tumor. In cancer, this molecule has a role in the detachment of tumor cells from other cells; adhesion to heterotypic cells and endothelial cells; and invasion and metastasis to other tissues.[77-79] Since there are some similarities in the mechanism of neural cell migration and tumor invasion regarding adhesion molecules and ECM changes,[80] we propose that high expression of ICAM1 in frontal/metopic groups is due to their neural crest origin and may suggest that these compartments are comprised of cells with greater migratory potential.

In addition to ICAM1, SULF1, PLAT, and TNC are all important factors in the composition of ECM and the differential expression of these transcripts in cranial compartments suggests that

ECM composition is differentially regulated during cranial development. Moreover, these genes may be among the factors that lead to early closure of the metopic suture relative to others. Each of these genes is expressed at higher levels in the metopic suture compared to other sutures. High expression of PLAT may cause changes in ECM allowing greater cellular migration. Similarly, ICAM1 facilitates adhesion of cells to heterotype cells and increases their motility; and SULF1 modulates the responsiveness of cell receptors to signaling pathways important in cell migration and osteogenesis. We suggest that these genes may modulate the ECM and induce mingling of neural crest-derived cells of frontal and metopic compartments which could result in early closure of the metopic suture.

Genes influential in proliferation are expressed in frontal/metopic group and genes important in differentiation are predominantly expressed in the parietal/sagittal group.

Our gene expression correlation analysis divided transcripts into two groups, one with higher levels of expression in the frontal and metopic compartments and the other one with higher levels of expression in the parietal and sagittal compartments. We found that these two groups of genes are also distinguished on the basis of function. Transcripts that promote proliferation are predominantly expressed in the frontal/metopic compartments and the transcripts that promote differentiation are predominantly expressed in the parietal/sagittal compartments.

Three of the most differentially expressed genes in our results were TFAP2 A and B (in frontal/metopic group) and FOXF2 (in parietal/sagittal groups). The literature indicates that the TFAP2 genes induce proliferation while the primary function of FOXF2 is differentiation.

Pfisterer et al. showed that a Tfap2a knock-out mouse mutant fails to close its neural tube. The mice had a cranial closure defect and there fibroblasts showed reduced proliferation, early differentiation and increased apoptosis. They suggested that this was due to the repression of genes involved in cell cycling and overexpression of genes related to the terminal differentiation.[81] Furthermore, increased expression of TFAP2A, B and C proteins is found in breast cancer [82, 83] cervical cancer [84] testicular cancer [85] myeloid leukemia [86] in association with a highly proliferative phenotype.

Inactivation of FoxF2 in a mouse intestinal mesoderm model leads to a reduction in ECM production and increased proliferation.[63] Similarly, investigation of the role of FOXF2 in breast, prostate and colon cancer has demonstrated that reduced expression of FOXF2 is associated with increased proliferation, reduction of ECM and a more invasive phenotype of the tumor.[87-91] Increased FOXF2 expression in the parietal bone and sagittal suture suggest increases differentiation.

Therefore, based on the gene expression in the calvaria we suggest that the frontal and metopic compartments have an increased potential for proliferation and reduced differentiation while the converse is true for the parietal and sagittal compartments. While there are few studies on the comparison of rodent frontal and parietal osteoblasts regarding these characteristics, most support our hypothesis that the frontal bone has a higher level of proliferation.[92-94] However, there are different opinions on the differentiation level of frontal and parietal bones. Xu et al.'s study reported a lower differentiation potential in frontal cells [92] while Li et al. reported increased differentiation in frontal cells.[93] Quarto et al. observed faster healing of frontal bone

in radiologic assessments which may be an explained by higher proliferative potential or enhanced differentiation of frontal osteoblasts.[94] Each of these investigations support our premise that the differential gene expression and cellular behavior is related to the origin of each cranial compartment.

Finally, we suggest that in suture complexes where two flanking bones and the intervening ISM are of neural crest origin that proliferation of osteoblasts of osteogenic front and their invasion into metopic ISM may cause early physiologic suture closure. This is not the case in sutures where the entire complex from paraxial mesoderm (sagittal suture) or the ones with ISM and flanking bones of different origins (coronal suture). We believe that metopic suture fuses early in development because frontal bone osteoblasts have high proliferative potential, low levels of differentiation, and highly migratory phenotype. In contrast we propose that the sagittal suture remains patent due to lower levels of proliferation and migration, and enhanced differentiation in the parietal osteogenic front and sagittal ISM. However, this may not be the case for all the sutures of neural crest origin, for instance labial side of premaxillary suture is fused at birth while the vomer side fuses later at the age of 15^{th}.[95]

Paracrine effects between compartments

In this study we evaluated the gene expression of each cell type in co-culture with two other cell types. Among the four co-culture sets (frontal, parietal, metopic and sagittal) larger changes were seen in frontal set and within this set the expression change was highest when frontal cells were in co-culture with sagittal cells. Some of the genes which were significantly different in comparison of co-cultured frontal cells with control frontal cells were also different in the

comparison of sagittal and frontal cells (without co-culture). The expression of these genes was substantially lower in both co-cultured frontal cells and sagittal cells compared to control frontal cells (Table S12). Based on this finding, when frontal cells are in co-culture with sagittal cells, their gene expression becomes more similar to sagittal cells compared to control frontal cells. These data suggest that frontal osteoblasts are most sensitive to secreted factors and most responsive to sagittal ISM cells.

One of the genes with a significant change in frontal cells co-cultured with sagittal cells is beta-actin (ACTB). Beta-actin is a part of the actin cytoskeleton responsible for cell shape, motility and cell-cell adhesion. All the environmental factors that control cell migration such as mechanical or biochemical (growth factor) factors affect cells through changes in cytoskeleton.[96] Because there is no variation in the mechanical stimuli between different co-cultures, the increase in expression of ACTB in frontal cells co-cultured with sagittal cells suggests that soluble factors from the sagittal ISM increase the expression of this frontal bone transcript involved in cell-cell adhesion. This suggests that secreted factors from sagittal cells increase cell-cell adhesion making the frontal bone cells take on a phenotype more similar to the parietal/sagittal group. Unlike co-culture experiments between the frontal and sagittal compartments, all other co-culture combination failed to identify significant paracrine effects.

.

Conclusion and future plan

The cranial compartments are of different embryonic origins. Our data suggests that the frontal and metopic compartments are of neural crest origin, and the parietal and sagittal compartments of paraxial mesoderm origin. In this study we aimed to evaluate gene expression and cell characteristics of cranial compartments related to their origins and to explore potential paracrine effects between these tissues.

Two analyses were performed on the expression array results. Paired comparison analysis demonstrated that gene expression the frontal and parietal bones are the most distinct compartments despite the fact that they are of the same tissue type (bone). Strikingly, comparison of gene expression between the frontal and metopic compartments and the parietal and sagittal compartments (bone vs. ISM) demonstrated more similar expression patterns. Correlation analysis revealed two groups of genes with highly correlated expression (group 1 and group 2). The genes in group 1 were highly correlated in the frontal and metopic compartments while those in group 2 were highly correlated in parietal and sagittal compartments. The segregation of frontal/metopic and parietal/sagittal groups based on this correlation analysis further supports the gene expression similarities of the frontal and metopic compartments and the parietal and sagittal compartments. The high level of expression of neural crest regulators in the frontal and metopic compartments suggests that one distinction between frontal/metopic and parietal/sagittal compartments is based on their embryonic origin. The expression profile suggests that the compartments derived from neural crest (frontal and metopic compartments)

may exhibit enhanced proliferation, reduced differentiation and tissue specific ECM composition when compared to parietal and sagittal compartments.

Our data suggest that the most significant differences between cranial compartments of like tissues are the expression of genes related to proliferation, differentiation and migration. In future studies we will evaluate these characteristics so that we can relate these cellular phenotypes to gene expression and better characterize the differences between the developing compartments of the calvaria. Unfortunately due to technical issues and our sample size the proliferation and differentiation assays could not support nor refute hypotheses suggested by our expression data. In the future studies, sufficient samples and improved methods will be used for this purpose. In order to evaluate the migration characteristics of the cells and their potential in mingling with other cell types during development we propose using Cre-ROSA26 systems to trace lineages in vitro. Wnt/Cre and Mesp/Cre mice co-cultures will be used to provide cell-cell contact of different cell types. In these co-cultures we can test our hypothesis about early fusion of metopic suture due to mingling of frontal and metopic cells.

References

1. Deckelbaum, R.A., et al., *Regulation of cranial morphogenesis and cell fate at the neural crest-mesoderm boundary by engrailed 1.* Development, 2012. **139**(7): p. 1346-58.
2. Moore, K.L., *The Developing Human Clinically Oriented Embryology*. 6 ed. 1998: Philadelphia, Saunders.
3. Cohen, M.M., Jr., *Craniosynostosis*. 2nd ed. 2000, New York: Oxford University Press.
4. Lajeunie, E., et al., *Genetic study of nonsyndromic coronal craniosynostosis.* Am J Med Genet, 1995. **55**(4): p. 500-4.
5. Kimonis, V., et al., *Genetics of craniosynostosis.* Semin Pediatr Neurol, 2007. **14**(3): p. 150-61.
6. Passos-Bueno, M.R., et al., *Genetics of craniosynostosis: genes, syndromes, mutations and genotype-phenotype correlations.* Front Oral Biol, 2008. **12**: p. 107-43.
7. Graham, J.M., Jr., R.J. Badura, and D.W. Smith, *Coronal craniostenosis: fetal head constraint as one possible cause.* Pediatrics, 1980. **65**(5): p. 995-9.
8. Graham, J.M., Jr., M. deSaxe, and D.W. Smith, *Sagittal craniostenosis: fetal head constraint as one possible cause.* J Pediatr, 1979. **95**(5 Pt 1): p. 747-50.
9. Graham, J.M., Jr. and D.W. Smith, *Metopic craniostenosis as a consequence of fetal head constraint: two interesting experiments of nature.* Pediatrics, 1980. **65**(5): p. 1000-2.
10. Biebermann, H., et al., *Constitutively activating TSH-receptor mutations as a molecular cause of non-autoimmune hyperthyroidism in childhood.* Langenbecks Arch Surg, 2000. **385**(6): p. 390-2.
11. de Lima, M.A., et al., *Congenital hyperthyroidism: autopsy report.* Rev Hosp Clin Fac Med Sao Paulo, 1999. **54**(3): p. 103-6.

12. Honein, M.A. and S.A. Rasmussen, *Further evidence for an association between maternal smoking and craniosynostosis.* Teratology, 2000. **62**(3): p. 145-6.

13. Reefhuis, J., et al., *Fertility treatments and craniosynostosis: California, Georgia, and Iowa, 1993-1997.* Pediatrics, 2003. **111**(5 Pt 2): p. 1163-6.

14. Lajeunie, E., et al., *Craniosynostosis and fetal exposure to sodium valproate.* J Neurosurg, 2001. **95**(5): p. 778-82.

15. Valentin, M., et al., *Trigonocephaly and valproate: a case report and review of literature.* Prenat Diagn, 2008. **28**(3): p. 259-61.

16. Kini, U., et al., *Etiological heterogeneity and clinical characteristics of metopic synostosis: Evidence from a tertiary craniofacial unit.* Am J Med Genet A, 2010. **152A**(6): p. 1383-9.

17. Ades, L.C., et al., *FBN1, TGFBR1, and the Marfan-craniosynostosis/mental retardation disorders revisited.* Am J Med Genet A, 2006. **140**(10): p. 1047-58.

18. Mefford, H.C., et al., *Copy number variation analysis in single-suture craniosynostosis: multiple rare variants including RUNX2 duplication in two cousins with metopic craniosynostosis.* Am J Med Genet A, 2010. **152A**(9): p. 2203-10.

19. Cunningham, M.L., et al., *IGF1R variants associated with isolated single suture craniosynostosis.* Am J Med Genet A, 2011. **155A**(1): p. 91-7.

20. Wilkie, A.O., *Craniosynostosis: genes and mechanisms.* Hum Mol Genet, 1997. **6**(10): p. 1647-56.

21. Sharma, V.P., et al., *Mutations in TCF12, encoding a basic helix-loop-helix partner of TWIST1, are a frequent cause of coronal craniosynostosis.* Nat Genet, 2013. **45**(3): p. 304-7.

22. Cunningham, M.L. and C.L. Heike, *Evaluation of the infant with an abnormal skull shape.* Curr Opin Pediatr, 2007. **19**(6): p. 645-51.

23. Seto, M.L., et al., *Isolated sagittal and coronal craniosynostosis associated with TWIST box mutations.* Am J Med Genet A, 2007. **143**(7): p. 678-86.

24. Greives, M.R., et al., *RUNX2 quadruplication: additional evidence toward a new form of syndromic craniosynostosis.* J Craniofac Surg, 2013. **24**(1): p. 126-9.

25. Jiang, X., et al., *Tissue origins and interactions in the mammalian skull vault.* Dev Biol, 2002. **241**(1): p. 106-16.

26. Yoshida, T., et al., *Cell lineage in mammalian craniofacial mesenchyme.* Mech Dev, 2008. **125**(9-10): p. 797-808.

27. Gagan, J.R., S.S. Tholpady, and R.C. Ogle, *Cellular dynamics and tissue interactions of the dura mater during head development.* Birth Defects Res C Embryo Today, 2007. **81**(4): p. 297-304.

28. Vu, H.L., et al., *The timing of physiologic closure of the metopic suture: a review of 159 patients using reconstructed 3D CT scans of the craniofacial region.* J Craniofac Surg, 2001. **12**(6): p. 527-32.

29. Levine, J.P., et al., *Studies in cranial suture biology: regional dura mater determines overlying suture biology.* Plast Reconstr Surg, 1998. **101**(6): p. 1441-7.

30. Bradley, J.P., et al., *Studies in cranial suture biology: in vitro cranial suture fusion.* Cleft Palate Craniofac J, 1996. **33**(2): p. 150-6.

31. Roth, D.A., et al., *Studies in cranial suture biology: part II. Role of the dura in cranial suture fusion.* Plast Reconstr Surg, 1996. **97**(4): p. 693-9.

32. Opperman, L.A., et al., *Cranial sutures require tissue interactions with dura mater to resist osseous obliteration in vitro.* J Bone Miner Res, 1995. **10**(12): p. 1978-87.

33. Kwan, M.D., et al., *Microarray analysis of the role of regional dura mater in cranial suture fate.* Plast Reconstr Surg, 2008. **122**(2): p. 389-99.

34. Greenwood, J., et al., *Intracellular domain of brain endothelial intercellular adhesion molecule-1 is essential for T lymphocyte-mediated signaling and migration.* J Immunol, 2003. **171**(4): p. 2099-108.

35. Warren, S.M., et al., *Regional dura mater differentially regulates osteoblast gene expression.* J Craniofac Surg, 2003. **14**(3): p. 363-70.

36. Opperman, L.A., A.A. Nolen, and R.C. Ogle, *TGF-beta 1, TGF-beta 2, and TGF-beta 3 exhibit distinct patterns of expression during cranial suture formation and obliteration in vivo and in vitro.* J Bone Miner Res, 1997. **12**(3): p. 301-10.

37. Opperman, L.A., et al., *Cranial suture obliteration is induced by removal of transforming growth factor (TGF)-beta 3 activity and prevented by removal of TGF-beta 2 activity from fetal rat calvaria in vitro.* J Craniofac Genet Dev Biol, 1999. **19**(3): p. 164-73.

38. Irizarry, R.A., et al., *Exploration, normalization, and summaries of high density oligonucleotide array probe level data.* Biostatistics, 2003. **4**(2): p. 249-64.

39. Ritchie, M.E., et al., *Empirical array quality weights in the analysis of microarray data.* BMC Bioinformatics, 2006. **7**: p. 261.

40. Smyth, G.K., *Linear models and empirical bayes methods for assessing differential expression in microarray experiments.* Stat Appl Genet Mol Biol, 2004. **3**: p. Article3.

41. Alter, O., P.O. Brown, and D. Botstein, *Singular value decomposition for genome-wide expression data processing and modeling.* Proc Natl Acad Sci U S A, 2000. **97**(18): p. 10101-6.

42. Stamper, B.D., et al., *Transcriptome correlation analysis identifies two unique craniosynostosis subtypes associated with IRS1 activation.* Physiol Genomics, 2012. **44**(23): p. 1154-63.

43. Milunsky, J.M., et al., *TFAP2A mutations result in branchio-oculo-facial syndrome.* Am J Hum Genet, 2008. **82**(5): p. 1171-7.

44. Zhao, F., et al., *Novel TFAP2B mutations that cause Char syndrome provide a genotype-phenotype correlation.* Am J Hum Genet, 2001. **69**(4): p. 695-703.

45. Dinwiddie, D.L., et al., *De novo frameshift mutation in ASXL3 in a patient with global developmental delay, microcephaly, and craniofacial anomalies.* BMC Med Genomics, 2013. **6**(1): p. 32.

46. Jochumsen, U., et al., *Mutation analysis of FOXF2 in patients with disorders of sex development (DSD) in combination with cleft palate.* Sex Dev, 2008. **2**(6): p. 302-8.

47. Stuhlmiller, T.J. and M.I. Garcia-Castro, *Current perspectives of the signaling pathways directing neural crest induction.* Cell Mol Life Sci, 2012. **69**(22): p. 3715-37.

48. Agrawal, M. and P.R. Brauer, *Urokinase-type plasminogen activator regulates cranial neural crest cell migration in vitro.* Dev Dyn, 1996. **207**(3): p. 281-90.

49. Erickson, C.A. and R.R. Isseroff, *Plasminogen activator activity is associated with neural crest cell motility in tissue culture.* J Exp Zool, 1989. **251**(2): p. 123-33.

50. Pietri, T., et al., *The human tissue plasminogen activator-Cre mouse: a new tool for targeting specifically neural crest cells and their derivatives in vivo.* Dev Biol, 2003. **259**(1): p. 176-87.

51. Powell, D.R., et al., *Prdm1a directly activates foxd3 and tfap2a during zebrafish neural crest specification.* Development, 2013. **140**(16): p. 3445-55.

52. Wang, T., et al., *Forkhead transcription factor Foxf2 (LUN)-deficient mice exhibit abnormal development of secondary palate.* Dev Biol, 2003. **259**(1): p. 83-94.

53. Zhang, Y., T. Luo, and T.D. Sargent, *Expression of TFAP2beta and TFAP2gamma genes in Xenopus laevis.* Gene Expr Patterns, 2006. **6**(6): p. 589-95.

54. Eckert, D., et al., *The AP-2 family of transcription factors.* Genome Biol, 2005. **6**(13): p. 246.

55. Chazaud, C., et al., *AP-2.2, a novel gene related to AP-2, is expressed in the forebrain, limbs and face during mouse embryogenesis.* Mech Dev, 1996. **54**(1): p. 83-94.

56. Mitchell, P.J., et al., *Transcription factor AP-2 is expressed in neural crest cell lineages during mouse embryogenesis.* Genes Dev, 1991. **5**(1): p. 105-19.

57. Moser, M., J. Ruschoff, and R. Buettner, *Comparative analysis of AP-2 alpha and AP-2 beta gene expression during murine embryogenesis.* Dev Dyn, 1997. **208**(1): p. 115-24.

58. ; Available from: http://omim.org/clinicalSynopsis/169100?search=Char syndrome&highlight=Char syndrome.

59. Schorle, H., et al., *Transcription factor AP-2 essential for cranial closure and craniofacial development.* Nature, 1996. **381**(6579): p. 235-8.

60. Zhang, J., et al., *Neural tube, skeletal and body wall defects in mice lacking transcription factor AP-2.* Nature, 1996. **381**(6579): p. 238-41.

61. Jeong, J., et al., *Hedgehog signaling in the neural crest cells regulates the patterning and growth of facial primordia.* Genes Dev, 2004. **18**(8): p. 937-51.

62. Betancur, P., M. Bronner-Fraser, and T. Sauka-Spengler, *Assembling neural crest regulatory circuits into a gene regulatory network.* Annu Rev Cell Dev Biol, 2010. **26**: p. 581-603.

63. Ormestad, M., et al., *Foxf1 and Foxf2 control murine gut development by limiting mesenchymal Wnt signaling and promoting extracellular matrix production.* Development, 2006. **133**(5): p. 833-43.

64. Aitola, M., et al., *Forkhead transcription factor FoxF2 is expressed in mesodermal tissues involved in epithelio-mesenchymal interactions.* Dev Dyn, 2000. **218**(1): p. 136-49.

65. Ormestad, M., J. Astorga, and P. Carlsson, *Differences in the embryonic expression patterns of mouse Foxf1 and -2 match their distinct mutant phenotypes.* Dev Dyn, 2004. **229**(2): p. 328-33.

66. Guiral, E.C., L. Faas, and M.E. Pownall, *Neural crest migration requires the activity of the extracellular sulphatases XtSulf1 and XtSulf2.* Dev Biol, 2010. **341**(2): p. 375-88.

67. Freeman, S.D., et al., *Extracellular regulation of developmental cell signaling by XtSulf1*. Dev Biol, 2008. **320**(2): p. 436-45.

68. Lum, D.H., et al., *Gene trap disruption of the mouse heparan sulfate 6-O-endosulfatase gene, Sulf2.* Mol Cell Biol, 2007. **27**(2): p. 678-88.

69. Menoud, P.A., S. Debrot, and J. Schowing, *Mouse neural crest cells secrete both urokinase-type and tissue-type plasminogen activators in vitro.* Development, 1989. **106**(4): p. 685-90.

70. Tucker, R.P., *Abnormal neural crest cell migration after the in vivo knockdown of tenascin-C expression with morpholino antisense oligonucleotides.* Dev Dyn, 2001. **222**(1): p. 115-9.

71. Tucker, R.P. and S.E. McKay, *The expression of tenascin by neural crest cells and glia.* Development, 1991. **112**(4): p. 1031-9.

72. Breau, M.A., et al., *Beta1 integrins are required for the invasion of the caecum and proximal hindgut by enteric neural crest cells.* Development, 2009. **136**(16): p. 2791-801.

73. Taneyhill, L.A., *To adhere or not to adhere: the role of Cadherins in neural crest development.* Cell Adh Migr, 2008. **2**(4): p. 223-30.

74. Degitz, K., L.J. Li, and S.W. Caughman, *Cloning and characterization of the 5'-transcriptional regulatory region of the human intercellular adhesion molecule 1 gene.* J Biol Chem, 1991. **266**(21): p. 14024-30.

75. Grether-Beck, S., et al., *Activation of transcription factor AP-2 mediates UVA radiation- and singlet oxygen-induced expression of the human intercellular adhesion molecule 1 gene.* Proc Natl Acad Sci U S A, 1996. **93**(25): p. 14586-91.

76. Duperray, A., et al., *Molecular identification of a novel fibrinogen binding site on the first domain of ICAM-1 regulating leukocyte-endothelium bridging.* J Biol Chem, 1997. **272**(1): p. 435-41.

77. Chen, P.C., et al., *CCN3 increases cell motility and ICAM-1 expression in prostate cancer cells.* Carcinogenesis, 2012. **33**(4): p. 937-45.

78. Collins, K.A. and W.L. White, *Intercellular adhesion molecule 1 (ICAM-1) and bcl-2 are differentially expressed in early evolving malignant melanoma.* Am J Dermatopathol, 1995. **17**(5): p. 429-38.

79. Lin, Y.M., et al., *IL-6 promotes ICAM-1 expression and cell motility in human osteosarcoma.* Cancer Lett, 2013. **328**(1): p. 135-43.

80. Powell, D.R., et al., *Riding the crest of the wave: parallels between the neural crest and cancer in epithelial-to-mesenchymal transition and migration.* Wiley Interdiscip Rev Syst Biol Med, 2013. **5**(4): p. 511-22.

81. Pfisterer, P., et al., *A subtractive gene expression screen suggests a role of transcription factor AP-2 alpha in control of proliferation and differentiation.* J Biol Chem, 2002. **277**(8): p. 6637-44.

82. Turner, B.C., et al., *Expression of AP-2 transcription factors in human breast cancer correlates with the regulation of multiple growth factor signalling pathways.* Cancer Res, 1998. **58**(23): p. 5466-72.

83. Bosher, J.M., et al., *A family of AP-2 proteins regulates c-erbB-2 expression in mammary carcinoma.* Oncogene, 1996. **13**(8): p. 1701-7.

84. Beger, M., et al., *Expression pattern of AP-2 transcription factors in cervical cancer cells and analysis of their influence on human papillomavirus oncogene transcription.* J Mol Med (Berl), 2001. **79**(5-6): p. 314-20.

85. Hoei-Hansen, C.E., et al., *Transcription factor AP-2gamma is a developmentally regulated marker of testicular carcinoma in situ and germ cell tumors.* Clin Cancer Res, 2004. **10**(24): p. 8521-30.

86. Ding, X., et al., *Transcription factor AP-2alpha regulates acute myeloid leukemia cell proliferation by influencing Hoxa gene expression.* Int J Biochem Cell Biol, 2013. **45**(8): p. 1647-56.

87. Shi, W., et al., *MicroRNA-301 mediates proliferation and invasion in human breast cancer.* Cancer Res, 2011. **71**(8): p. 2926-37.

88. van der Heul-Nieuwenhuijsen, L., N.F. Dits, and G. Jenster, *Gene expression of forkhead transcription factors in the normal and diseased human prostate.* BJU Int, 2009. **103**(11): p. 1574-80.

89. Hirata, H., et al., *MicroRNA-182-5p promotes cell invasion and proliferation by down regulating FOXF2, RECK and MTSS1 genes in human prostate cancer.* PLoS One, 2013. **8**(1): p. e55502.

90. Nik, A.M., et al., *Foxf2 in intestinal fibroblasts reduces numbers of Lgr5(+) stem cells and adenoma formation by inhibiting Wnt signaling.* Gastroenterology, 2013. **144**(5): p. 1001-11.

91. Kong, P.Z., et al., *Decreased FOXF2 mRNA expression indicates early-onset metastasis and poor prognosis for breast cancer patients with histological grade II tumor.* PLoS One, 2013. **8**(4): p. e61591.

92. Xu, Y., et al., *Molecular and cellular characterization of mouse calvarial osteoblasts derived from neural crest and paraxial mesoderm.* Plast Reconstr Surg, 2007. **120**(7): p. 1783-95.

93. Li, S., N. Quarto, and M.T. Longaker, *Activation of FGF signaling mediates proliferative and osteogenic differences between neural crest derived frontal and mesoderm parietal derived bone.* PLoS One, 2010. **5**(11): p. e14033.

94. Quarto, N., et al., *Origin matters: differences in embryonic tissue origin and Wnt signaling determine the osteogenic potential and healing capacity of frontal and parietal calvarial bones.* J Bone Miner Res, 2010. **25**(7): p. 1680-94.

95. Barteczko, K. and M. Jacob, *A re-evaluation of the premaxillary bone in humans.* Anat Embryol (Berl), 2004. **207**(6): p. 417-37.

96. Mitra, S.K., D.A. Hanson, and D.D. Schlaepfer, *Focal adhesion kinase: in command and control of cell motility.* Nat Rev Mol Cell Biol, 2005. **6**(1): p. 56-68.

Supplemets

Table S1: Expression difference of control frontal and parietal cells

symbol	gene name	unigene	F_F - P_P fold Δ	p-value
TFAP2B	transcription factor AP-2 beta (activating enhancer binding protein 2 beta)	Hs.33102	3.78	7.6E-04
MAB21L1	mab-21-like 1 (C. elegans)	Hs.584776	3.68	1.1E-03
SHC4	SHC (Src homology 2 domain containing) family, member 4	Hs.642615	3.08	4.2E-03
MTRNR2L2	MT-RNR2-like 2	Hs.666077	3.07	7.5E-05
DNAJC6	DnaJ (Hsp40) homolog, subfamily C, member 6	Hs.647643	2.6	5.9E-05
SLC24A3	solute carrier family 24 (sodium/potassium/calcium exchanger), member 3	Hs.654790	2.44	8.6E-04
DYSF	dysferlin, limb girdle muscular dystrophy 2B (autosomal recessive)	Hs.252180	2.31	4.5E-05
MT1L	metallothionein 1L (gene/pseudogene)	Hs.647358	2.23	7.4E-03
C5orf46	chromosome 5 open reading frame 46	Hs.660038	2.21	9.4E-05
KRTAP2-3	keratin associated protein 2-3	Hs.406714	2.16	9.1E-03
AGTR1	angiotensin II receptor, type 1	Hs.477887	2.06	2.8E-03
DRAM1	DNA-damage regulated autophagy modulator 1	Hs.525634	1.92	3.2E-03
SLC16A3	solute carrier family 16, member 3 (monocarboxylic acid transporter 4)	Hs.500761	1.9	1.9E-03
NPPB	natriuretic peptide B	Hs.219140	1.86	1.8E-05
MGC40069	uncharacterized protein MGC40069	Hs.369380	1.82	6.8E-04
MT1G	metallothionein 1G	Hs.433391	1.78	1.7E-03
CCBE1	collagen and calcium binding EGF domains 1	Hs.34333	1.77	5.9E-03
MAP3K5	mitogen-activated protein kinase kinase kinase 5	Hs.186486	1.75	6.8E-06
BAIAP2L1	BAI1-associated protein 2-like 1	Hs.656063	1.75	5.3E-05
IVNS1ABP	influenza virus NS1A binding protein	Hs.497183	1.73	1.1E-03
ZNF735	zinc finger protein 735	Hs.723116	1.73	1.6E-03
SLCO3A1	solute carrier organic anion transporter family, member 3A1	Hs.311187	1.73	5.4E-04
PPAPDC1A	phosphatidic acid phosphatase type 2 domain containing 1A	Hs.40479	1.72	2.4E-03
SPANXN4	SPANX family, member N4	Hs.535082	1.71	3.3E-04
DKK1	dickkopf 1 homolog (Xenopus laevis)	Hs.40499	1.71	7.4E-03
SHOX2	short stature homeobox 2	Hs.55967	1.7	2.7E-03
FLT1	fms-related tyrosine kinase 1	Hs.594454	1.69	8.3E-04
FMN2	formin 2	Hs.24889	1.69	3.3E-06
GAS6	growth arrest-specific 6	Hs.646346	1.67	6.6E-03
MT1F	metallothionein 1F	Hs.513626	1.67	3.3E-03
ADM	adrenomedullin	Hs.441047	1.67	1.4E-03
AMIGO2	adhesion molecule with Ig-like domain 2	Hs.121520	1.66	3.4E-03
ENTPD1	ectonucleoside triphosphate diphosphohydrolase 1	Hs.722260	1.66	7.0E-03
MT1X	metallothionein 1X	Hs.374950	1.65	5.6E-04
NEDD4L	neural precursor cell expressed, developmentally down-regulated 4-like, E3 ubiquitin protein ligase	Hs.185677	1.65	5.5E-03
CCNL1	cyclin L1	Hs.4859	1.63	1.4E-03
PDCD1LG2	programmed cell death 1 ligand 2	Hs.532279	1.62	2.7E-03
CCDC81	coiled-coil domain containing 81	Hs.144913	1.62	8.1E-03
GPR183	G protein-coupled receptor 183	Hs.784	1.61	5.1E-05
MEGF6	multiple EGF-like-domains 6	Hs.593645	1.6	2.5E-03
NTF3	neurotrophin 3	Hs.99171	1.59	6.8E-03
FAM169A	family with sequence similarity 169, member A	Hs.91662	1.57	7.6E-03
ZNF732	zinc finger protein 732	Hs.698668	1.55	9.8E-03
EFHD1	EF-hand domain family, member D1	Hs.516769	1.54	5.2E-04
CCL7	chemokine (C-C motif) ligand 7	Hs.251526	1.54	2.4E-03
C5orf60	chromosome 5 open reading frame 60	Hs.558748	1.52	5.9E-03
KRTAP3-2	keratin associated protein 3-2	Hs.307026	1.51	9.6E-03
DPCR1	diffuse panbronchiolitis critical region 1	Hs.631993	1.5	5.0E-03
CELA2B	chymotrypsin-like elastase family, member 2B	Hs.631871	1.5	8.9E-03
AFAP1L1	actin filament associated protein 1-like 1	Hs.483793	1.5	1.6E-03
LOC100508227	uncharacterized LOC100508227	Hs.689354	-1.5	1.9E-03
HECW2	HECT, C2 and WW domain containing E3 ubiquitin protein ligase 2	Hs.654742	-1.5	9.0E-03
BTBD8	BTB (POZ) domain containing 8	Hs.676102	-1.51	5.0E-04
TEK	TEK tyrosine kinase, endothelial	Hs.89640	-1.51	7.1E-03
LOC100127910	uncharacterized LOC100127910	Hs.647752	-1.52	3.3E-03
PRSS12	protease, serine, 12 (neurotrypsin, motopsin)	Hs.445857	-1.53	8.8E-04
ZIC1	Zic family member 1	Hs.598590	-1.53	1.5E-03
LURAP1L	leucine rich adaptor protein 1-like	Hs.445356	-1.53	6.5E-03

Table S1 continued

LAMP3	lysosomal-associated membrane protein 3	Hs.518448	-1.54	3.2E-04
KRTAP13-4	keratin associated protein 13-4	Hs.553677	-1.55	1.4E-03
PDE4D	phosphodiesterase 4D, cAMP-specific	Hs.117545	-1.55	4.8E-04
LRRC4C	leucine rich repeat containing 4C	Hs.135736	-1.56	7.1E-03
FOXP2	forkhead box P2	Hs.282787	-1.56	8.1E-04
OLFML1	olfactomedin-like 1	Hs.503500	-1.57	8.8E-03
ST6GALNAC3	ST6 (alpha-N-acetyl-neuraminyl-2,3-beta-galactosyl-1,3)-N-acetylgalactosaminide alpha-2,6-sialyltransferase 3	Hs.337040	-1.58	2.5E-03
PLCE1	phospholipase C, epsilon 1	Hs.655033	-1.58	3.5E-03
ZIC4	Zic family member 4	Hs.415766	-1.6	4.4E-04
IGFN1	immunoglobulin-like and fibronectin type III domain containing 1	Hs.519024	-1.6	1.3E-03
FAM155A	family with sequence similarity 155, member A	Hs.535394	-1.6	2.2E-03
ABCA9	ATP-binding cassette, sub-family A (ABC1), member 9	Hs.131686	-1.6	5.0E-03
KCNT2	potassium channel, subfamily T, member 2	Hs.657046	-1.61	2.9E-05
MFAP4	microfibrillar-associated protein 4	Hs.296049	-1.61	3.2E-03
KLHL4	kelch-like family member 4	Hs.49075	-1.61	6.3E-04
KIAA1107	KIAA1107	Hs.21554	-1.61	7.1E-05
MGC24103	uncharacterized MGC24103	Hs.664877	-1.61	1.9E-03
GPC6	glypican 6	Hs.444329	-1.63	1.1E-03
CDH6	cadherin 6, type 2, K-cadherin (fetal kidney)	Hs.124776	-1.63	9.4E-04
TOX	thymocyte selection-associated high mobility group box	Hs.491805	-1.63	9.9E-03
RDH10	retinol dehydrogenase 10 (all-trans)	Hs.244940	-1.66	1.9E-03
TNFRSF11B	tumor necrosis factor receptor superfamily, member 11b	Hs.81791	-1.69	1.0E-03
MXRA5	matrix-remodelling associated 5	Hs.369422	-1.69	5.6E-03
ARHGAP28	Rho GTPase activating protein 28	Hs.183114	-1.69	2.1E-04
FOXF2	forkhead box F2	Hs.484423	-1.71	8.8E-04
ST6GAL1	ST6 beta-galactosamide alpha-2,6-sialyltranferase 1	Hs.207459	-1.71	2.4E-04
HSPB6	heat shock protein, alpha-crystallin-related, B6	Hs.534538	-1.74	1.0E-03
TNC	tenascin C	Hs.143250	-1.74	1.6E-04
FGL2	fibrinogen-like 2	Hs.520989	-1.76	6.2E-03
PDE5A	phosphodiesterase 5A, cGMP-specific	Hs.647971	-1.78	7.2E-06
DCLK1	doublecortin-like kinase 1	Hs.507755	-1.79	7.5E-04
SMPDL3A	sphingomyelin phosphodiesterase, acid-like 3A	Hs.486357	-1.82	1.2E-04
C3orf62	chromosome 3 open reading frame 62	Hs.403828	-1.85	8.0E-03
TCEAL3	transcription elongation factor A (SII)-like 3	Hs.311776	-1.87	1.7E-03
SLC2A12	solute carrier family 2 (facilitated glucose transporter), member 12	Hs.486508	-1.92	1.1E-05
IFI44	interferon-induced protein 44	Hs.82316	-1.95	9.3E-05
ANK3	ankyrin 3, node of Ranvier (ankyrin G)	Hs.499725	-1.98	1.1E-03
KCNA1	potassium voltage-gated channel, shaker-related subfamily, member 1 (episodic ataxia with myokymia)	Hs.416139	-1.99	1.4E-04
ST6GALNAC5	ST6 (alpha-N-acetyl-neuraminyl-2,3-beta-galactosyl-1,3)-N-acetylgalactosaminide alpha-2,6-sialyltransferase 5	Hs.303609	-2.08	8.0E-04
SLC7A2	solute carrier family 7 (cationic amino acid transporter, y+ system), member 2	Hs.448520	-2.19	7.9E-03
LGI1	leucine-rich, glioma inactivated 1	Hs.533670	-2.21	1.0E-03
ABCA8	ATP-binding cassette, sub-family A (ABC1), member 8	Hs.58351	-2.21	1.8E-05
MAB21L2	mab-21-like 2 (C. elegans)	Hs.584852	-2.36	4.2E-03
IQGAP2	IQ motif containing GTPase activating protein 2	Hs.291030	-2.78	4.6E-05
OGN	osteoglycin	Hs.109439	-4.93	1.1E-04

Table S2: Expression difference of control frontal and sagittal cells

symbol	gene name	unigene	F_F-S_S fold Δ	p-value
TFAP2B	transcription factor AP-2 beta (activating enhancer binding protein 2 beta)	Hs.33102	4.52	1.8E-04
OR51E1	olfactory receptor, family 51, subfamily E, member 1	Hs.470038	3.11	1.8E-03
MTRNR2L2	MT-RNR2-like 2	Hs.666077	3.07	7.3E-05
C5orf46	chromosome 5 open reading frame 46	Hs.660038	2.47	1.4E-05
DNAJC6	DnaJ (Hsp40) homolog, subfamily C, member 6	Hs.647643	2.45	1.4E-04
RGS7	regulator of G-protein signaling 7	Hs.655739	2.32	1.5E-03
MGC40069	uncharacterized protein MGC40069	Hs.369380	2.19	2.4E-05
DYSF	dysferlin, limb girdle muscular dystrophy 2B (autosomal recessive)	Hs.252180	2.14	1.5E-04
OXTR	oxytocin receptor	Hs.2820	2.09	3.1E-03
SPANXN4	SPANX family, member N4	Hs.535082	2	1.0E-05
DSC2	desmocollin 2	Hs.95612	1.99	6.4E-03
DRAM1	DNA-damage regulated autophagy modulator 1	Hs.525634	1.98	2.2E-03
NPPB	natriuretic peptide B	Hs.219140	1.84	2.5E-05
PDLIM1	PDZ and LIM domain 1	Hs.368525	1.81	8.6E-03
C5orf60	chromosome 5 open reading frame 60	Hs.558748	1.78	2.8E-04
KRTAP3-2	keratin associated protein 3-2	Hs.307026	1.78	5.2E-04
AMIGO2	adhesion molecule with Ig-like domain 2	Hs.121520	1.78	1.1E-03
DPCR1	diffuse panbronchiolitis critical region 1	Hs.631993	1.78	1.6E-04
IL1B	interleukin 1, beta	Hs.126256	1.77	3.1E-03
HNF1B	HNF1 homeobox B	Hs.191144	1.75	2.3E-03
FHDC1	FH2 domain containing 1	Hs.132629	1.75	4.8E-03
MEGF6	multiple EGF-like-domains 6	Hs.593645	1.75	4.6E-04
TFAP2A	transcription factor AP-2 alpha (activating enhancer binding protein 2 alpha)	Hs.519880	1.73	1.3E-03
ENTPD1	ectonucleoside triphosphate diphosphohydrolase 1	Hs.722260	1.65	7.9E-03
LRRC3C	leucine rich repeat containing 3C	Hs.145136	1.64	8.8E-03
IFNA13	interferon, alpha 13	Hs.533471	1.62	2.1E-04
ICAM1	intercellular adhesion molecule 1	Hs.643447	1.62	8.2E-05
AFAP1L1	actin filament associated protein 1-like 1	Hs.483793	1.6	3.2E-04
EFHD1	EF-hand domain family, member D1	Hs.516769	1.58	2.7E-04
CCL7	chemokine (C-C motif) ligand 7	Hs.251526	1.57	1.5E-03
IGHG1	immunoglobulin heavy constant gamma 1 (G1m marker)	Hs.510635	1.56	2.4E-03
IVNS1ABP	influenza virus NS1A binding protein	Hs.497183	1.55	7.8E-03
MT1H	metallothionein 1H	Hs.438462	1.54	4.5E-03
LOC440563	heterogeneous nuclear ribonucleoprotein C-like	Hs.711869	1.52	1.5E-04
SLCO3A1	solute carrier organic anion transporter family, member 3A1	Hs.311187	1.52	6.4E-03
GALNT14	UDP-N-acetyl-alpha-D-galactosamine:polypeptide N-acetylgalactosaminyltransferase 14 (GalNAc-T14)	Hs.468058	1.52	5.6E-04
MAP3K5	mitogen-activated protein kinase kinase kinase 5	Hs.186486	1.51	4.4E-04
CD274	CD274 molecule	Hs.521989	1.51	1.3E-03
NIPSNAP3B	nipsnap homolog 3B (C. elegans)	Hs.429294	-1.5	9.6E-03
LDB2	LIM domain binding 2	Hs.714330	-1.51	3.6E-04
TMOD2	tropomodulin 2 (neuronal)	Hs.513734	-1.51	2.0E-03
ST6GALNAC3	ST6 (alpha-N-acetyl-neuraminyl-2,3-beta-galactosyl-1,3)-N-acetylgalactosaminide alpha-2,6-sialyltransferase 3	Hs.337040	-1.52	5.3E-03
CASK	calcium/calmodulin-dependent serine protein kinase (MAGUK family)	Hs.495984	-1.52	2.2E-03
CCDC34	coiled-coil domain containing 34	Hs.143733	-1.52	4.0E-03
HNRNPA1L2	heterogeneous nuclear ribonucleoprotein A1-like 2	Hs.447506	-1.52	4.6E-03
TEX9	testis expressed 9	Hs.511476	-1.53	1.3E-04
ADD3	adducin 3 (gamma)	Hs.501012	-1.53	2.3E-05
LRRN3	leucine rich repeat neuronal 3	Hs.3781	-1.54	8.2E-03
PDCD4	programmed cell death 4 (neoplastic transformation inhibitor)	Hs.711490	-1.54	5.8E-03
DCN	decorin	Hs.156316	-1.55	1.3E-05
ADAMTS3	ADAM metallopeptidase with thrombospondin type 1 motif, 3	Hs.590919	-1.55	2.8E-03
TNC	tenascin C	Hs.143250	-1.55	1.9E-03
CACNA2D3	calcium channel, voltage-dependent, alpha 2/delta subunit 3	Hs.656687	-1.55	4.7E-04
HECW2	HECT, C2 and WW domain containing E3 ubiquitin protein ligase 2	Hs.654742	-1.57	4.4E-03
PRSS12	protease, serine, 12 (neurotrypsin, motopsin)	Hs.445857	-1.57	4.2E-04
GRB14	growth factor receptor-bound protein 14	Hs.411881	-1.58	8.7E-04
MSX2	msh homeobox 2	Hs.89404	-1.59	3.5E-04
PROS1	protein S (alpha)	Hs.64016	-1.61	3.9E-03

Table S2 continued

VSTM4	V-set and transmembrane domain containing 4	Hs.522928	-1.62	1.9E-04
MFAP4	microfibrillar-associated protein 4	Hs.296049	-1.62	2.6E-03
IRAK3	interleukin-1 receptor-associated kinase 3	Hs.369265	-1.62	9.4E-03
MEIS2	Meis homeobox 2	Hs.510989	-1.64	6.2E-04
CCDC152	coiled-coil domain containing 152	Hs.275775	-1.65	9.0E-03
ZNF678	zinc finger protein 678	Hs.30323	-1.65	2.0E-04
KCNT2	potassium channel, subfamily T, member 2	Hs.657046	-1.66	9.5E-06
ADAMTSL3	ADAMTS-like 3	Hs.459162	-1.67	4.4E-03
LURAP1L	leucine rich adaptor protein 1-like	Hs.445356	-1.67	1.3E-03
ZNF681	zinc finger protein 681	Hs.399952	-1.68	1.4E-03
TMEM200A	transmembrane protein 200A	Hs.591341	-1.68	6.4E-05
HSPB6	heat shock protein, alpha-crystallin-related, B6	Hs.534538	-1.69	1.7E-03
IFI44	interferon-induced protein 44	Hs.82316	-1.72	1.0E-03
DCLK1	doublecortin-like kinase 1	Hs.507755	-1.73	1.4E-03
SCN2A	sodium channel, voltage-gated, type II, alpha subunit	Hs.93485	-1.74	1.9E-03
PDE5A	phosphodiesterase 5A, cGMP-specific	Hs.647971	-1.75	1.0E-05
TNFRSF11B	tumor necrosis factor receptor superfamily, member 11b	Hs.81791	-1.77	3.8E-04
MXRA5	matrix-remodelling associated 5	Hs.369422	-1.8	2.2E-03
ESM1	endothelial cell-specific molecule 1	Hs.129944	-1.83	3.5E-03
ABCA8	ATP-binding cassette, sub-family A (ABC1), member 8	Hs.58351	-1.84	5.4E-04
CTHRC1	collagen triple helix repeat containing 1	Hs.405614	-1.86	7.4E-04
FLRT3	fibronectin leucine rich transmembrane protein 3	Hs.41296	-1.91	1.2E-03
MKX	mohawk homeobox	Hs.128193	-1.92	2.6E-03
DES	desmin	Hs.594952	-1.93	4.2E-03
LRRC4C	leucine rich repeat containing 4C	Hs.135736	-1.94	1.4E-04
LGI1	leucine-rich, glioma inactivated 1	Hs.533670	-1.94	4.9E-03
KLHL4	kelch-like family member 4	Hs.49075	-1.95	7.1E-06
PLA2G4A	phospholipase A2, group IVA (cytosolic, calcium-dependent)	Hs.497200	-1.96	4.2E-04
CMKLR1	chemokine-like receptor 1	Hs.197143	-2	1.4E-04
IL26	interleukin 26	Hs.272350	-2.04	5.0E-04
FGL2	fibrinogen-like 2	Hs.520989	-2.09	5.5E-04
FAM155A	family with sequence similarity 155, member A	Hs.535394	-2.15	4.7E-06
EMB	embigin	Hs.561411	-2.19	9.6E-06
TCEAL3	transcription elongation factor A (SII)-like 3	Hs.311776	-2.2	1.4E-04
IQGAP2	IQ motif containing GTPase activating protein 2	Hs.291030	-2.24	8.1E-04
ST6GALNAC5	ST6 (alpha-N-acetyl-neuraminyl-2,3-beta-galactosyl-1,3)-N-acetylgalactosaminide alpha-2,6-sialyltransferase 5	Hs.303609	-2.28	2.1E-04
SLC7A2	solute carrier family 7 (cationic amino acid transporter, y+ system), member 2	Hs.448520	-2.43	3.1E-03
MTRNR2L8	MT-RNR2-like 8	Hs.717003	-3.57	8.0E-03
SCN3A	sodium channel, voltage-gated, type III, alpha subunit	Hs.435274	-4.25	3.2E-04
MAB21L2	mab-21-like 2 (C. elegans)	Hs.584852	-4.27	8.7E-06
OGN	osteoglycin	Hs.109439	-6.84	7.4E-06

Table S3: Expression differennce of control metopic and parietal cells

symbol	gene name	unigene	M_M-P_P fold Δ	p-value
TFAP2B	transcription factor AP-2 beta (activating enhancer binding protein 2 beta)	Hs.33102	5.85	2.1E-05
MAB21L1	mab-21-like 1 (C. elegans)	Hs.584776	3.87	7.4E-04
MBOAT1	membrane bound O-acyltransferase domain containing 1	Hs.377830	2.57	9.1E-05
AGTR1	angiotensin II receptor, type 1	Hs.477887	2.52	2.2E-04
DNAJC6	DnaJ (Hsp40) homolog, subfamily C, member 6	Hs.647643	2.5	1.1E-04
MRAP2	melanocortin 2 receptor accessory protein 2	Hs.370055	2.21	7.3E-03
MTRNR2L2	MT-RNR2-like 2	Hs.666077	2.13	4.7E-03
FAM105A	family with sequence similarity 105, member A	Hs.155085	2.08	1.2E-03
ABI3BP	ABI family, member 3 (NESH) binding protein	Hs.477015	2.04	5.3E-04
SHCBP1	SHC SH2-domain binding protein 1	Hs.123253	1.95	8.7E-03
PPAPDC1A	phosphatidic acid phosphatase type 2 domain containing 1A	Hs.40479	1.9	4.3E-04
CCBE1	collagen and calcium binding EGF domains 1	Hs.34333	1.9	2.2E-03
BRIP1	BRCA1 interacting protein C-terminal helicase 1	Hs.128903	1.83	9.0E-03
DRAM1	DNA-damage regulated autophagy modulator 1	Hs.525634	1.79	8.1E-03
ENPP2	ectonucleotide pyrophosphatase/phosphodiesterase 2	Hs.190977	1.77	3.0E-03
TFAP2A	transcription factor AP-2 alpha (activating enhancer binding protein 2 alpha)	Hs.519880	1.74	1.2E-03
IVNS1ABP	influenza virus NS1A binding protein	Hs.497183	1.74	1.1E-03
ASXL3	additional sex combs like 3 (Drosophila)	Hs.464876	1.73	3.1E-03
EBF3	early B-cell factor 3	Hs.591374	1.67	1.4E-03
MT1F	metallothionein 1F	Hs.513626	1.66	3.5E-03
MT1G	metallothionein 1G	Hs.433391	1.65	5.8E-03
CDH3	cadherin 3, type 1, P-cadherin (placental)	Hs.191842	1.64	3.2E-04
MT1X	metallothionein 1X	Hs.374950	1.61	9.0E-04
ZNF735	zinc finger protein 735	Hs.723116	1.61	5.7E-03
GMNN	geminin, DNA replication inhibitor	Hs.234896	1.6	3.4E-03
SHOX2	short stature homeobox 2	Hs.55967	1.57	9.2E-03
MDC1	mediator of DNA-damage checkpoint 1	Hs.653495	1.56	7.0E-03
ANP32E	acidic (leucine-rich) nuclear phosphoprotein 32 family, member E	Hs.656466	1.53	6.3E-03
MYPN	myopalladin	Hs.55205	1.53	3.0E-05
VIT	vitrin	Hs.137415	1.52	3.9E-03
MT1A	metallothionein 1A	Hs.655199	1.5	2.4E-03
HECW2	HECT, C2 and WW domain containing E3 ubiquitin protein ligase 2	Hs.654742	-1.51	8.0E-03
ARMC9	armadillo repeat containing 9	Hs.471610	-1.52	3.0E-05
SASH1	SAM and SH3 domain containing 1	Hs.193133	-1.52	8.1E-03
KLHL4	kelch-like family member 4	Hs.49075	-1.53	2.1E-03
LOC100286914	putative uncharacterized protein C20orf69-like	NA	-1.53	1.7E-03
HSPB6	heat shock protein, alpha-crystallin-related, B6	Hs.534538	-1.53	9.3E-03
SPTBN1	spectrin, beta, non-erythrocytic 1	Hs.503178	-1.56	5.3E-03
SLC2A12	solute carrier family 2 (facilitated glucose transporter), member 12	Hs.486508	-1.56	1.3E-03
PDK3	pyruvate dehydrogenase kinase, isozyme 3	Hs.296031	-1.6	9.0E-03
IGFN1	immunoglobulin-like and fibronectin type III domain containing 1	Hs.519024	-1.61	1.2E-03
ST6GAL1	ST6 beta-galactosamide alpha-2,6-sialyltranferase 1	Hs.207459	-1.62	8.6E-04
KCNA1	potassium voltage-gated channel, shaker-related subfamily, member 1 (episodic ataxia with myokymia)	Hs.416139	-1.63	4.6E-03
TNFRSF11B	tumor necrosis factor receptor superfamily, member 11b	Hs.81791	-1.64	1.7E-03
PKP2	plakophilin 2	Hs.164384	-1.68	4.9E-03
FOXF2	forkhead box F2	Hs.484423	-1.72	7.5E-04
SLC9A7	solute carrier family 9, subfamily A (NHE7, cation proton antiporter 7), member 7	Hs.91389	-1.75	1.2E-04
FRY	furry homolog (Drosophila)	Hs.507669	-1.75	8.8E-04
C3orf62	chromosome 3 open reading frame 62	Hs.403828	-1.91	5.4E-03
KAL1	Kallmann syndrome 1 sequence	Hs.521869	-2.02	3.6E-03
TNC	tenascin C	Hs.143250	-2.05	3.5E-06
LUZP2	leucine zipper protein 2	Hs.144138	-2.13	5.5E-04
ANK3	ankyrin 3, node of Ranvier (ankyrin G)	Hs.499725	-2.24	1.7E-04
MAB21L2	mab-21-like 2 (C. elegans)	Hs.584852	-3.2	2.0E-04

Table S4: Expression difference of control metopic and sagittal cells

symbol	gene name	unigene	M_M-S_S fold Δ	p-value
TFAP2B	transcription factor AP-2 beta (activating enhancer binding protein 2 beta)	Hs.33102	7	4.4E-06
MRAP2	melanocortin 2 receptor accessory protein 2	Hs.370055	2.43	3.1E-03
DNAJC6	DnaJ (Hsp40) homolog, subfamily C, member 6	Hs.647643	2.35	2.5E-04
MTRNR2L2	MT-RNR2-like 2	Hs.666077	2.13	4.6E-03
ABI3BP	ABI family, member 3 (NESH) binding protein	Hs.477015	2.13	2.6E-04
AGTR1	angiotensin II receptor, type 1	Hs.477887	2.07	2.7E-03
FAM105A	family with sequence similarity 105, member A	Hs.155085	2.03	1.7E-03
TFAP2A	transcription factor AP-2 alpha (activating enhancer binding protein 2 alpha)	Hs.519880	1.97	1.2E-04
TBX15	T-box 15	Hs.146196	1.95	1.9E-04
MBOAT1	membrane bound O-acyltransferase domain containing 1	Hs.377830	1.86	6.2E-03
DRAM1	DNA-damage regulated autophagy modulator 1	Hs.525634	1.84	5.7E-03
TRIM51	tripartite motif-containing 51	Hs.326734	1.8	1.6E-03
ASXL3	additional sex combs like 3 (Drosophila)	Hs.464876	1.78	2.0E-03
SLC16A14	solute carrier family 16, member 14 (monocarboxylic acid transporter 14)	Hs.504317	1.77	2.2E-03
MGC40069	uncharacterized protein MGC40069	Hs.369380	1.76	1.3E-03
FHDC1	FH2 domain containing 1	Hs.132629	1.7	6.7E-03
ARGFX	arginine-fifty homeobox	Hs.224976	1.62	5.9E-04
PPAPDC1A	phosphatidic acid phosphatase type 2 domain containing 1A	Hs.40479	1.61	7.0E-03
SLC1A3	solute carrier family 1 (glial high affinity glutamate transporter), member 3	Hs.481918	1.6	8.0E-03
VIT	vitrin	Hs.137415	1.6	1.6E-03
GOLGA6L4	golgin A6 family-like 4	Hs.498345	1.56	3.9E-03
CDH3	cadherin 3, type 1, P-cadherin (placental)	Hs.191842	1.56	1.2E-03
IVNS1ABP	influenza virus NS1A binding protein	Hs.497183	1.55	7.8E-03
IGHG1	immunoglobulin heavy constant gamma 1 (G1m marker)	Hs.510635	1.53	3.5E-03
ZNF763	zinc finger protein 763	Hs.646386	-1.5	2.9E-03
SLC9A7	solute carrier family 9, subfamily A (NHE7, cation proton antiporter 7), member 7	Hs.91389	-1.51	2.7E-04
VSTM4	V-set and transmembrane domain containing 4	Hs.522928	-1.52	8.6E-04
KCTD16	potassium channel tetramerisation domain containing 16	Hs.661870	-1.53	1.5E-04
MAP3K7CL	MAP3K7 C-terminal like	Hs.222802	-1.54	9.6E-05
FAM155A	family with sequence similarity 155, member A	Hs.535394	-1.55	3.9E-03
SPTBN1	spectrin, beta, non-erythrocytic 1	Hs.503178	-1.55	5.4E-03
HECW2	HECT, C2 and WW domain containing E3 ubiquitin protein ligase 2	Hs.654742	-1.58	3.9E-03
ZNF610	zinc finger protein 610	Hs.147025	-1.63	5.4E-04
PCDHB8	protocadherin beta 8	Hs.283803	-1.64	3.0E-03
FGD4	FYVE, RhoGEF and PH domain containing 4	Hs.117835	-1.64	5.0E-05
IRAK3	interleukin-1 receptor-associated kinase 3	Hs.369265	-1.64	8.1E-03
PLA2G4A	phospholipase A2, group IVA (cytosolic, calcium-dependent)	Hs.497200	-1.72	3.5E-03
TNFRSF11B	tumor necrosis factor receptor superfamily, member 11b	Hs.81791	-1.72	6.6E-04
CMKLR1	chemokine-like receptor 1	Hs.197143	-1.78	1.2E-03
SERPINB2	serpin peptidase inhibitor, clade B (ovalbumin), member 2	Hs.594481	-1.79	5.6E-03
TNC	tenascin C	Hs.143250	-1.83	5.2E-05
KLHL4	kelch-like family member 4	Hs.49075	-1.84	2.7E-05
KAL1	Kallmann syndrome 1 sequence	Hs.521869	-1.85	9.8E-03
LUZP2	leucine zipper protein 2	Hs.144138	-1.87	3.3E-03
SLC9A7	solute carrier family 9, subfamily A (NHE7, cation proton antiporter 7), member 7	Hs.91389	-1.89	1.9E-05
PALMD	palmdelphin	Hs.483993	-2.21	6.8E-04
SCN3A	sodium channel, voltage-gated, type III, alpha subunit	Hs.435274	-3.08	3.9E-03
MAB21L2	mab-21-like 2 (C. elegans)	Hs.584852	-5.78	3.0E-07

Table S5: Expression difference of control frontal and metopic cells

symbol	gene name	unigene	F_F-M_M fold Δ	p-value
ANKRD1	ankyrin repeat domain 1 (cardiac muscle)	Hs.448589	2.25	5.2E-03
C5orf46	chromosome 5 open reading frame 46	Hs.660038	2.19	1.1E-04
DYSF	dysferlin, limb girdle muscular dystrophy 2B (autosomal recessive)	Hs.252180	2	4.6E-04
SLC16A3	solute carrier family 16, member 3 (monocarboxylic acid transporter 4)	Hs.500761	1.84	2.9E-03
MYH11	myosin, heavy chain 11, smooth muscle	Hs.460109	1.82	5.7E-03
FHOD3	formin homology 2 domain containing 3	Hs.630884	1.7	9.4E-03
NPPB	natriuretic peptide B	Hs.219140	1.68	2.1E-04
SLC9A7	solute carrier family 9, subfamily A (NHE7, cation proton antiporter 7), member 7	Hs.91389	1.59	1.0E-03
LYN	v-yes-1 Yamaguchi sarcoma viral related oncogene homolog	Hs.491767	1.55	4.4E-04
PCDHB8	protocadherin beta 8	Hs.283803	1.54	7.8E-03
AFAP1L1	actin filament associated protein 1-like 1	Hs.483793	1.51	1.4E-03
MAP3K5	mitogen-activated protein kinase kinase kinase 5	Hs.186486	1.5	5.4E-04
EMB	embigin	Hs.561411	-1.52	9.0E-03
RARB	retinoic acid receptor, beta	Hs.654490	-1.55	2.2E-04
ARHGAP28	Rho GTPase activating protein 28	Hs.183114	-1.55	1.5E-03
PTPRD	protein tyrosine phosphatase, receptor type, D	Hs.446083	-1.58	9.4E-04
EBF3	early B-cell factor 3	Hs.591374	-1.62	2.6E-03
MXRA5	matrix-remodelling associated 5	Hs.369422	-1.65	8.3E-03
DCLK1	doublecortin-like kinase 1	Hs.507755	-1.65	3.0E-03
ABCA8	ATP-binding cassette, sub-family A (ABC1), member 8	Hs.58351	-1.7	2.3E-03
IQGAP2	IQ motif containing GTPase activating protein 2	Hs.291030	-1.92	5.8E-03
OGN	osteoglycin	Hs.109439	-3.36	2.3E-03

Table S6: Expression difference of control parietal and sagittal cells

symbol	gene name	unigene	P_P-S_S fold Δ	p-value
CACNA2D3	calcium channel, voltage-dependent, alpha 2/delta subunit 3	Hs.656687	-1.6	2.2E-04
CCDC30	coiled-coil domain containing 30	Hs.729640	-1.52	5.3E-03
CCNL1	cyclin L1	Hs.4859	-1.61	1.7E-03
EMB	embigin	Hs.561411	-1.64	2.6E-03
EN1	engrailed homeobox 1	Hs.271977	-1.58	9.5E-03
FIBIN	fin bud initiation factor homolog (zebrafish)	Hs.712718	-1.63	2.4E-03
IGFN1	immunoglobulin-like and fibronectin type III domain containing 1	Hs.519024	1.53	3.2E-03
NTF3	neurotrophin 3	Hs.99171	-1.62	4.9E-03
PDCD1LG2	programmed cell death 1 ligand 2	Hs.532279	-1.53	7.7E-03
PTGS2	prostaglandin-endoperoxide synthase 2 (prostaglandin G/H synthase and cyclooxygenase)	Hs.196384	-1.62	1.2E-03
SERPINI1	serpin peptidase inhibitor, clade I (neuroserpin), member 1	Hs.478153	-1.7	6.3E-03
TBX15	T-box 15	Hs.146196	1.63	4.2E-03
XG	Xg blood group	Hs.179675	-2.6	9.2E-03

Table S7: Expression change of frontal cells in co-culture with metopic cells

symbol	genename	unigene	M_F-F_F fold Δ	p-value
TCEAL3	transcription elongation factor A (SII)-like 3	Hs.311776	1.99	6.6E-04
HLA-DPB1	major histocompatibility complex, class II, DP beta 1	Hs.485130	1.56	7.1E-03
SNRPN	small nuclear ribonucleoprotein polypeptide N	;Hs.621316;	1.51	7.2E-03
CCNL1	cyclin L1	Hs.4859	-1.54	4.1E-03
MT1H	metallothionein 1H	Hs.438462	-1.59	2.6E-03
KRTAP3-2	keratin associated protein 3-2	Hs.307026	-1.61	3.3E-03
SPANXN4	SPANX family, member N4	Hs.535082	-1.67	5.8E-04
MGC40069	uncharacterized protein MGC40069	Hs.369380	-1.86	4.7E-04
MTRNR2L2	MT-RNR2-like 2	Hs.666077	-2.23	2.9E-03

Table S8: Expression change of frontal cells in co-culture with sagittal cells

symbol	genename	unigene	S_F-F_F fold Δ	p-value
MTRNR2L8	MT-RNR2-like 8	Hs.717003	3.45	9.7E-03
TCEAL3	transcription elongation factor A (SII)-like 3	Hs.311776	2.13	2.3E-04
ACTB	actin, beta	Hs.520640	1.86	6.3E-03
HLA-DPB1	major histocompatibility complex, class II, DP beta 1	Hs.485130	1.53	9.6E-03
IGHA1	immunoglobulin heavy constant alpha 1	Hs.699841	1.5	7.1E-03
ZNF716	zinc finger protein 716	Hs.533121	-1.52	5.3E-03
LAIR2	leukocyte-associated immunoglobulin-like receptor 2	Hs.43803	-1.53	6.6E-03
CTAG2	cancer/testis antigen 2	Hs.87225	-1.53	4.8E-03
TEX13A	testis expressed 13A	Hs.567543	-1.55	2.8E-05
C5orf60	chromosome 5 open reading frame 60	Hs.558748	-1.57	3.5E-03
CELA2B	chymotrypsin-like elastase family, member 2B	Hs.631871	-1.58	3.7E-03
CTAGE9	CTAGE family, member 9	Hs.632613	-1.59	4.4E-04
OPCML	opioid binding protein/cell adhesion molecule-like	Hs.4817	-1.62	7.1E-05
KRTAP3-3	keratin associated protein 3-3	Hs.662759	-1.66	3.1E-04
KRTAP3-2	keratin associated protein 3-2	Hs.307026	-1.72	9.2E-04
DPCR1	diffuse panbronchiolitis critical region 1	Hs.631993	-1.81	1.1E-04
SPANXN4	SPANX family, member N4	Hs.535082	-2.05	5.7E-06
MGC40069	uncharacterized protein MGC40069	Hs.369380	-2.31	8.2E-06
MTRNR2L2	MT-RNR2-like 2	Hs.666077	-2.81	2.1E-04

Table S9: Group 1 correlated genes

symbol	unigene	symbol	unigene	symbol	unigene	symbol	unigene
ABI3BP	Hs.477015	CD274	Hs.521989	KCNIP1	Hs.484111	PVALB	Hs.295449
ACADM	Hs.445040	CDH8	Hs.368322	KRT34	Hs.296942	QPCT	Hs.79033
ASXL3	Hs.464876	CELA2B	Hs.631871	KRTAP1-5	Hs.534499	RASGRP1	Hs.591127
CDH3	Hs.191842	CELF2	Hs.309288	KRTAP3-2	Hs.307026	RGS7	Hs.655739
DNAJC6	Hs.647643	CENPV	Hs.433422	KRTAP3-3	Hs.662759	S100A7	Hs.112408
DNER	Hs.234074	CFHR3	Hs.709217	KRTAP4-8	Hs.307019	SCN9A	Hs.439145
DRAM1	Hs.525634	CLDN1	Hs.439060	LIPH	Hs.68864	SDPR	Hs.26530
ENTPD1	Hs.722260	CLSTN2	Hs.158529	LOC440905	Hs.469918	SGIP1	Hs.132121
FAM105A	Hs.155085	CNTN1	Hs.143434	LRRC32	Hs.151641	SH3RF2	Hs.443728
GPR183	Hs.784	CNTNAP3	Hs.128474	LRRC3C	Hs.145136	SHC4	Hs.642615
ICAM1	Hs.643447	CNTNAP3B	Hs.521495	LYN	Hs.491767	SHOX2	Hs.55967
IGHG1	Hs.510635	CPXM1	Hs.659346	LYVE1	Hs.655332	SIX2	Hs.101937
IL11	Hs.467304	CTAG2	Hs.87225	MAL2	Hs.201083	SLC16A14	Hs.504317
IVNS1ABP	Hs.497183	CTAGE9	Hs.632613	MAMDC2	Hs.547172	SLC1A3	Hs.481918
KRT7	Hs.411501	CYP4X1	Hs.439760	MAP3K5	Hs.186486	SLC20A1	Hs.187946
LDOC1	Hs.45231	DCC	Hs.162025	MBOAT1	Hs.377830	SLC24A3	Hs.654790
MAB21L1	Hs.584776	DCDC2	Hs.61345	MBOAT2	Hs.467634	SLC29A1	Hs.25450
MRAP2	Hs.370055	DIO2	Hs.202354	MDC1	Hs.653495	SLC2A1	Hs.473721
MT1F	Hs.513626	DIRAS2	Hs.165636	MEGF6	Hs.593645	SLCO3A1	Hs.311187
MT1X	Hs.374950	DPCR1	Hs.631993	MFAP3L	Hs.593942	SLITRK6	Hs.525105
MTRNR2L2	Hs.666077	DSC2	Hs.95612	MGAM	Hs.122785	SNRPN	Hs.555970
MYPN	Hs.55205	DSC3	Hs.41690	MGST1	Hs.389700	SPANXN1	Hs.551270
NGF	Hs.2561	DSG2	Hs.412597	MT1A	Hs.655199	SPANXN4	Hs.535082
PLAT	Hs.491582	DYSF	Hs.252180	MT1G	Hs.433391	SPOCD1	Hs.62604
PPAPDC1A	Hs.40479	EBI3	Hs.501452	MT1H	Hs.438462	SRGN	Hs.1908
SULF1	Hs.409602	ECSCR	Hs.483538	MT1L	Hs.647358	STARD4	Hs.93842
TFAP2A	Hs.519880	EDN1	Hs.511899	MTHFD2L	Hs.721011	STRA6	Hs.24553
TFAP2B	Hs.33102	EFHD1	Hs.516769	MYH11	Hs.460109	SYDE2	Hs.670497
ACTBL2	Hs.482167	ELOVL2	Hs.656436	MYO1D	Hs.602063	SYT16	Hs.404139
ADA	Hs.654536	ENPP2	Hs.190977	MYOCD	Hs.567641	TBX15	Hs.146196
ADAM29	Hs.126838	FAM101B	Hs.345588	NEDD4L	Hs.185677	TFAP2C	Hs.473152
ADAMTS5	Hs.58324	FAM169A	Hs.91662	NFASC	Hs.13349	TLL1	Hs.106513
ADCY5	Hs.593292	FAT2	Hs.591255	NOX4	Hs.371036	TLL2	Hs.154296
ADM	Hs.441047	FGF5	Hs.37055	NPPB	Hs.219140	TMEM217	Hs.520101
AFAP1L1	Hs.483793	FHDC1	Hs.132629	NRK	Hs.209527	TRIM24	Hs.490287
AGMO	Hs.670634	FHOD3	Hs.630884	NRP2	Hs.471200	TRPC6	Hs.159003
AGTR1	Hs.477887	FLT1	Hs.594454	OGFRL1	Hs.648434	TSPAN2	Hs.310458
AIM1	Hs.643590	FMN2	Hs.24889	OR2T11	Hs.626619	UBL4B	Hs.374027
ALX1	Hs.41683	FRZB	Hs.128453	OR4A5	Hs.554531	VIT	Hs.137415
ALX3	Hs.669953	GALNT14	Hs.468058	OR51E1	Hs.470038	YME1L1	Hs.499145
AMIGO2	Hs.121520	GPC5	Hs.655675	OR8H2	Hs.553744	ZNF732	Hs.698668
ANKRD1	Hs.448589	GPR56	Hs.513633	OVCH2	Hs.532475	ZNF735	Hs.723116
ANKRD28	Hs.335239	GREM1	Hs.40098	OXTR	Hs.2820		
ANXA3	Hs.480042	GRPR	Hs.567282	PADI2	Hs.33455		
APBB1IP	Hs.310421	GUCY1A3	Hs.24258	PAX3	Hs.42146		
ARGFX	Hs.224976	GUCY1B3	Hs.77890	PCDH10	Hs.192859		
ARHGAP15	Hs.171011	HBEGF	Hs.592942	PCDH7	Hs.479439		
ASS1	Hs.160786	HGF	Hs.396530	PDE1A	Hs.191046		
BAIAP2L1	Hs.656063	HIST1H2BD	Hs.591797	PDLIM1	Hs.368525		
BCCIP	Hs.370292	HIST1H3H	Hs.591778	PERP	Hs.201446		
C5orf46	Hs.660038	HIST1H4F	Hs.247816	PGK1	Hs.78771		
C5orf60	Hs.558748	HNF1B	Hs.191144	PLXDC1	Hs.125036		
CACNG4	Hs.514423	IFNA13	Hs.533471	PPARGC1A	Hs.527078		
CCBE1	Hs.34333	IL1B	Hs.126256	PPIF	Hs.381072		
CCDC68	Hs.120790	IL23A	Hs.382212	PRG4	Hs.647723		
CCDC81	Hs.144913	IL8	Hs.624	PRPS1	Hs.56		
CCL7	Hs.251526	ITGA3	Hs.265829	PTPLA	Hs.114062		
CCNL1	Hs.4859	ITIH2	Hs.75285	PTPRZ1	Hs.489824		

Table S10: Group 2 correlated genes

symbol	unigene	symbol	unigene	symbol	unigene	symbol	unigene	symbol	unigene	symbol	unigene
ADH1B	Hs.4	CCDC34	Hs.143733	GDF15	Hs.616962	MKX	Hs.128193	RRP7B	Hs.534041	ZIC1	Hs.598590
ARHGEF35	Hs.534621	CDH6	Hs.124776	GPC6	Hs.444329	MMP2	Hs.513617	RSPO2	Hs.444834	ZIC4	Hs.415766
BTBD8	Hs.676102	CDR1	Hs.446675	GPR1	Hs.184907	MPHOSPH6	Hs.344400	S100A4	Hs.654444	ZNF429	Hs.572567
C3orf62	Hs.403828	CENPP	Hs.713775	GRB14	Hs.411881	MST4	Hs.444247	SASH1	Hs.193133	ZNF430	Hs.729202
CCND2	Hs.376071	CETN4P	Hs.647968	GRIA3	Hs.377070	MSX2	Hs.89404	SCARNA15	Hs.743895	ZNF486	Hs.590991
CD55	Hs.126517	CMKLR1	Hs.197143	GRIK1	Hs.664641	MSX2P1	Hs.381329	SCN2A	Hs.93485	ZNF610	Hs.147025
FAM129A	Hs.518662	COL14A1	Hs.409662	HAPLN1	Hs.2799	MTHFD1	Hs.652308	SCN3A	Hs.435274	ZNF675	Hs.264345
FOXF2	Hs.484423	COL1A2	Hs.489142	HHIP	Hs.507991	MTRNR2L8	Hs.717003	SCN8A	Hs.436550	ZNF678	Hs.30323
FXYD1	Hs.442498	COLEC12	Hs.464422	HIST2H3D	Hs.712062	MXRA5	Hs.369422	SEC11C	Hs.45107	ZNF681	Hs.399952
GEM	Hs.654463	CRISPLD1	Hs.436542	HNRNPA1L2	Hs.447506	MYOZ2	Hs.732122	SEMG1	Hs.1968	ZNF711	Hs.326801
HECW2	Hs.654742	CRLF1	Hs.114948	HNRNPA3	Hs.516539	NFATC2IP	Hs.513470	SEPP1	Hs.275775	ZNF763	Hs.646386
HSPB6	Hs.534538	CTHRC1	Hs.405614	HSPA9	Hs.184233	NFE2L3	Hs.404741	SERPINB2	Hs.594481		
KCNT2	Hs.657046	CTSK	Hs.632466	IFI44	Hs.82316	NFIL3	Hs.79334	SERPINI1	Hs.478153		
KIAA1107	Hs.21554	CX3CL1	Hs.531668	IFITM1	Hs.458414	NIPSNAP3B	Hs.429294	SFRP4	Hs.658169		
KLHL4	Hs.49075	CXorf40A	Hs.534641	IGFN1	Hs.519024	NOV	Hs.235935	SFTA1P	Hs.31562		
MAB21L2	Hs.584852	DCHS1	Hs.199850	IGHA1	Hs.699841	NPY1R	Hs.519057	SGCD	Hs.387207		
MFAP4	Hs.296049	DCLK1	Hs.507755	IL26	Hs.272350	NR2F2	Hs.347991	SHOX	Hs.105932		
MYLIP	Hs.484738	DCN	Hs.156316	IQGAP2	Hs.291030	NTRK2	Hs.494312	SIPA1L2	Hs.268774		
PDE5A	Hs.647971	DENND2C	Hs.654928	IRAK3	Hs.369265	OCLN	Hs.592605	SLC16A9	Hs.499709		
PRSS12	Hs.445857	DEPTOR	Hs.112981	ITGA8	Hs.171311	OGN	Hs.109439	SLC2A12	Hs.486508		
ST6GALNAC5	Hs.303609	DES	Hs.594952	KAL1	Hs.521869	OLFML1	Hs.503500	SLC7A2	Hs.448520		
TNC	Hs.143250	DHRS3	Hs.289347	KBTBD8	Hs.116665	OLR1	Hs.412484	SLC7A3	Hs.175220		
TNFRSF11B	Hs.81791	DIP2A-IT1	Hs.737163	KCNA1	Hs.416139	OMD	Hs.94070	SLC9A7	Hs.91389		
ABCA8	Hs.58351	DKFZP686I15	Hs.720158	KCNG1	Hs.118695	OSTN	Hs.526794	SLITRK3	Hs.101745		
ABCA9	Hs.131686	DSCC1	Hs.315167	KCNMB1	Hs.484099	PALMD	Hs.483993	SMOC2	Hs.487200		
ABCC9	Hs.732701	EEF1A1	Hs.535192	KCTD16	Hs.661870	PCDHB12	Hs.429820	SMPDL3A	Hs.486357		
ACTB	Hs.520640	EGFL6	Hs.12844	KIAA1324L	Hs.208093	PCDHB13	Hs.283803	SPTBN1	Hs.503178		
ACTR6	Hs.115088	ELFN1	Hs.42896	KIAA1462	Hs.533953	PCDHB14	Hs.658497	SSX2IP	Hs.22587		
ADAMTS15	Hs.534221	ELN	Hs.647061	KITLG	Hs.1048	PCDHB16	Hs.147674	ST6GAL1	Hs.207459		
ADAMTS3	Hs.590919	ELTD1	Hs.132314	KRTAP13-4	Hs.553677	PCDHB8	Hs.283803	ST6GALNAC2	Hs.592105		
ADAMTSL3	Hs.459162	EMB	Hs.561411	LALBA	Hs.72938	PDCD4	Hs.711490	ST6GALNAC3	Hs.337040		
ADD3	Hs.501012	EPGN	Hs.401237	LAMA2	Hs.200841	PDE4D	Hs.117545	SULT1B1	Hs.129742		
AGAP11	Hs.511787	EPHA5	Hs.654492	LAMP3	Hs.518448	PDGFRA	Hs.74615	SULT1E1	Hs.479898		
AK5	Hs.559718	EPHA7	Hs.73962	LDB2	Hs.714330	PDGFRL	Hs.458573	TAS2R19	Hs.687025		
ALDH8A1	Hs.486520	EREG	Hs.115263	LEPREL1	Hs.374191	PDK3	Hs.296031	TAS2R20	Hs.686384		
AMTN	Hs.453069	ESF1	Hs.369284	LGI1	Hs.533670	PDLIM3	Hs.701364	TAS2R30	Hs.679464		
AMZ2P1	Hs.396447	ESM1	Hs.129944	LGR5	Hs.658889	PGAP1	Hs.229988	TCEAL3	Hs.311776		
ANGPT2	Hs.583870	EYA4	Hs.596680	LHFPL2	Hs.670094	PITX2	Hs.643588	TDRD1	Hs.333132		
ANGPTL2	Hs.653262	FAM151B	Hs.338182	LIMCH1	Hs.335163	PKDCC	Hs.408542	TEK	Hs.89640		
ANK3	Hs.499725	FAM155A	Hs.535394	LMCD1	Hs.475353	PKP2	Hs.164384	TEX9	Hs.511476		
ANKRD29	Hs.374774	FAM198B	Hs.567498	LPAR1	Hs.126667	PLA2G4A	Hs.497200	TGM2	Hs.517033		
ANPEP	Hs.1239	FAM43A	Hs.435080	LPPR4	Hs.13245	PLCE1	Hs.655033	TIMP3	Hs.644633		
AP1AR	Hs.435991	FGD4	Hs.117835	LRP4	Hs.4930	PLCL1	Hs.153322	TMED5	Hs.482873		
ARHGAP28	Hs.183114	FGF16	Hs.666364	LRRC17	Hs.567412	POPDC3	Hs.458336	TMEM200A	Hs.591341		
ARL6	Hs.373801	FGF9	Hs.111	LRRC37A3	Hs.551962	PPIP5K1	Hs.156814	TMOD2	Hs.513734		
ARMC9	Hs.471610	FGL2	Hs.520989	LRRC4C	Hs.135736	PRAMEF3	Hs.558935	TNXA	Hs.708061		
ASPN	Hs.435655	FIBIN	Hs.712718	LRRN3	Hs.3781	PRKG1	Hs.407535	TNXB	Hs.485104		
BACH1	Hs.154276	FLRT3	Hs.41296	LURAP1L	Hs.445356	PROS1	Hs.64016	TOX	Hs.491805		
BCRP3	Hs.531306	FMOD	Hs.519168	LUZP2	Hs.144138	PTGS2	Hs.196384	TPPP3	Hs.534458		
BLID	Hs.686109	FNDC1	Hs.520525	LY96	Hs.726603	PTPRD	Hs.446083	TRIM48	Hs.195715		
C1orf110	Hs.407631	FOS	Hs.731317	MAGOHB	Hs.104650	PTX3	Hs.591286	TRPC4	Hs.262960		
C9orf64	Hs.208914	FOXP1-IT1	Hs.655773	MALAT1	Hs.621695	RAB27B	Hs.25318	TXNIP	Hs.533977		
CACNA2D3	Hs.656687	FOXP2	Hs.282787	MAN1A1	Hs.102788	RAD51AP1	Hs.730696	USP1	Hs.35086		
CALCRL	Hs.470882	FRY	Hs.507669	MAP3K8	Hs.432453	RAET1L	Hs.558659	VCAN	Hs.643801		
CASK	Hs.495984	FST	Hs.9914	MDGA1	Hs.437993	RARB	Hs.654490	VSTM4	Hs.522928		
CCDC102B	Hs.280781	GAP43	Hs.134974	MEIS2	Hs.510989	RDH10	Hs.244940	XAF1	Hs.441975		
CCDC112	Hs.436121	GBP3	Hs.720167	MEOX2	Hs.170355	RPL21	Hs.381123	YY2	Hs.673601		
CCDC152	Hs.275775	GCA	Hs.377894	METTL7A	Hs.744021	RPLP0P2	Hs.502733	ZDHHC15	Hs.253211		

Table S11: Group 3 correlated genes

symbol	unigene	symbol	unigene	symbol	unigene
PBK	Hs.104741	GINS2	Hs.433180	TBX3	Hs.744016
SGOL1	Hs.105153	CKAP2L	Hs.434250	CENPE	Hs.75573
HUNK	Hs.109437	VEGFC	Hs.435215	DLGAP5	Hs.77695
RFC3	Hs.115474	TPMT	Hs.444319	KIAA0101	Hs.81892
APCDD1L	Hs.119286	DEPDC1	Hs.445098	CKS2	Hs.83758
ASPM	Hs.121028	NCAPG	Hs.446201	CDKN3	Hs.84113
SHCBP1	Hs.123253	ACOT2	Hs.446685	SKA3	Hs.88523
BRIP1	Hs.128903	BNC1	Hs.459153	KIF11	Hs.8878
HIST1H1B	Hs.131956	CD97	Hs.466039	FLJ46906	Hs.92290
LOC10050639	Hs.132168	BUB1	Hs.469649	UBE2C	Hs.93002
SKA1	Hs.134726	CDCA7	Hs.470654	OLFML3	Hs.9315
HIST1H4B	Hs.143080	LXN	Hs.478067	NTF3	Hs.99171
CEP55	Hs.14559	SFRP2	Hs.481022	ESCO2	Hs.99480
HIST1H1A	Hs.150206	HS3ST3B1	Hs.48384		
TOP2A	Hs.156346	CENPF	Hs.497741		
HAS2	Hs.159226	KCNK2	Hs.497745		
TTK	Hs.169840	EXO1	Hs.498248		
BHLHE40	Hs.171825	SLC16A3	Hs.500761		
XG	Hs.179675	LOC283299	Hs.501825		
CASC5	Hs.181855	NNAT	Hs.504703		
HIST1H2BM	Hs.182432	CRISPLD2	Hs.513779		
MELK	Hs.184339	TK1	Hs.515122		
FAM111B	Hs.186579	UBE2T	Hs.5199		
CCNB2	Hs.194698	CDC20	Hs.524947		
SLC38A5	Hs.195155	CENPK	Hs.529778		
C18orf54	Hs.208701	PDCD1LG2	Hs.532279		
ITGB3	Hs.218040	SERPINF1	Hs.532768		
LAMP5	Hs.22920	HIST1H2AI	Hs.534035		
GMNN	Hs.234896	FAM72D	Hs.535577		
CCNB1	Hs.23960	PTPRQ	Hs.539284		
KIF20B	Hs.240	FAM180A	Hs.55200		
HIST1H3G	Hs.247813	WNT2	Hs.567356		
HIST1H4D	Hs.248179	MLF1IP	Hs.575032		
NET1	Hs.25155	CCNA2	Hs.58974		
STC1	Hs.25590	ARHGAP11A	Hs.591130		
PRUNE2	Hs.262857	EBF3	Hs.591374		
KIF23	Hs.270845	CLMP	Hs.591949		
EN1	Hs.271977	PLK1	Hs.592049		
KIF18A	Hs.301052	FAM64A	Hs.592116		
SH2D4A	Hs.303208	NUSAP1	Hs.615092		
NCAPH	Hs.308045	ANLN	Hs.62180		
KIF14	Hs.3104	CENPH	Hs.631967		
SNX5	Hs.316890	WNT5A	Hs.643085		
CDCA2	Hs.33366	GAS6	Hs.646346		
BEX1	Hs.334370	NUF2	Hs.651950		
CENPI	Hs.348920	HELLS	Hs.655830		
OR5P2	Hs.351824	ANP32E	Hs.656466		
PRC1	Hs.366401	DTL	Hs.656473		
TYMS	Hs.369762	KIF15	Hs.658939		
CADM1	Hs.370510	ARHGAP11B	Hs.659621		
PTN	Hs.371249	KCND3	Hs.666367		
DKK1	Hs.40499	ZNF724P	Hs.675814		
NEIL3	Hs.405467	MKI67	Hs.689823		
CRABP2	Hs.405662	KIF20A	Hs.718626		
CDC6	Hs.405958	CCDC30	Hs.729640		
NDC80	Hs.414407	CDK1	Hs.732435		
HNMT	Hs.42151	HMMR	Hs.740467		
LYAR	Hs.425427	CHRM2	Hs.743546		

Table S12: Shared genes of two comparisons: Co-cultured frontal cells vs. control frontal cells and sagittal cells vs. frontal cells

symbol	S_F-F_F fold Δ	p-value	S_S-F_F fold Δ	p-value
C5orf60	-1.57	3.5E-03	-1.78	2.8E-04
DPCR1	-1.81	1.1E-04	-1.78	1.6E-04
KRTAP3-2	-1.72	9.2E-04	-1.78	5.2E-04
MGC40069	-2.31	8.2E-06	-2.19	2.4E-05
MTRNR2L2	-2.81	2.1E-04	-3.07	7.3E-05
MTRNR2L8	3.45	9.7E-03	3.57	8.0E-03
SPANXN4	-2.05	5.7E-06	-2	1.0E-05
TCEAL3	2.13	2.3E-04	2.2	1.4E-04